

Climatology of short-period tidal oscillations in  
the upper atmosphere

Kjetil Landgraaf Ekern

June 16, 2013



### **Abstract**

This project has used data from a SKiYMET radar located at Dragvoll, Trondheim, to find the individual components of atmospheric tidal waves. Through least squares fitting there was found components of both the quaterdiurnal and terdiurnal, the climatology of these components were then analyzed. The terdiurnal tide was the main focus of this project, and found to have amplitudes that are at times comparable and even greater than the amplitude of the diurnal and the semidiurnal tide.



### **Acknowledgements**

I would like to give a special thanks to my supervisor Patrick Joseph Espy, for giving me an interesting project. Also for giving me the freedom and time to figure things out on my own, while always having the time to answer any of my questions.



# Contents

<b>1</b>	<b>Introduction</b>	<b>7</b>
<b>2</b>	<b>Atmospheric tidal waves</b>	<b>9</b>
<b>3</b>	<b>The SKiYMET meteor radar</b>	<b>12</b>
<b>4</b>	<b>Method</b>	<b>18</b>
<b>5</b>	<b>Results</b>	<b>20</b>
<b>6</b>	<b>Discussion</b>	<b>37</b>
<b>7</b>	<b>Conclusion</b>	<b>41</b>
<b>A</b>	<b>Matlab code</b>	<b>45</b>
A.1	Main program file and control file when finding the amplitudes and phases . . . . .	45
A.2	Codes to sort the data and fit U's and V's . . . . .	51
A.3	Example of fitting function to get the amplitudes and phases. . .	55



# List of Figures

2.1	Illustration of the different Fourier components of the wind (black) that are produced the heating (red) . . . . .	10
3.1	Example of the meteor distribution. Picture from the atmospheric groups webpage [11] . . . . .	13
3.2	Overview picture of the setup of the SKiYMET radar at Dragvoll. Picture from [9] . . . . .	14
3.3	Example of output file from the SKiYMET meteor radar. Data used in this project: Time, Ht: Height, Vrad: Line of sight velocity, Theta: zenith angle, Phi0: Azimuth angle, ambig: ambiguity level . . . . .	15
3.4	Example of the graphic of the zonal and meridional wind that can be found at the atmospheric groups homepage [11] . . . . .	16
5.1	(a) Significant amplitudes for the diurnal wave from the period September 10th to April 30th. (b) $2\sigma$ error of the amplitudes. . .	21
5.2	Corresponding $2\sigma$ to the amplitudes of the diurnal in figure 5.1 .	22
5.3	(a) Significant amplitudes found for the semidiurnal tidal wave in the period from September 10th 2012 until April 30th 2013. (b) $2\sigma$ error of the amplitudes. . . . .	26
5.4	Corresponding phases to the amplitudes of the semidiurnal in figure 5.3. . . . .	27
5.5	(a) Significant amplitudes found for the terdiurnal tidal wave in the period September 10th 2012 until April 30th 2013. (b) corresponding $2\sigma$ error. . . . .	28
5.6	Corresponding phases to the amplitudes of the terdiurnal in figure 5. . . . .	29
5.7	(a) Significant amplitudes found for the 6-hour tidal wave in the period from September 10th 2012 until April 30th 2013. (b) $2\sigma$ error of the amplitudes. . . . .	30
5.8	phase for the amplitudes found in figure 5.7 . . . . .	31
5.9	The background wind at different points in the atmosphere, fitted in the code as a constant. . . . .	32
5.10	Scatter plot with the amplitudes of the terdiurnal plotted against the amplitude of the diurnal tide. (a) Zonal, (b) Meridional. . . .	33

5.11	Scatter plot with the amplitude of the terdiurnal plotted against the amplitude of the semidiurnal. (a) zonal, (b) meridional . . .	34
5.12	scatter plot of the terdiurnal amplitude against the semidiurnal+diurnal. (a) Zonal, (b) meridional . . . . .	35
6.1	Plot of the data and the fits for 81-84 km, 09.Oct 2012 . . . . .	39
6.2	Caption for FourierU-93-96 . . . . .	40

# Chapter 1

## Introduction

The analysis of the climatology of the higher frequency components of the tidal oscillations in the upper atmosphere is done to get a better understanding of atmospheric phenomena. If this part of the atmosphere can be better understood and modeled, it would be possible to include these models in for example weather/climate models and possibly get more accurate weather predictions. Phenomena in the lower atmosphere and the upper atmosphere can interact with each other and it is therefore important to have a better understanding of both in order to fully understand how the atmosphere will behave and react to different events like solar flares and other changes in heating/cooling. It has previously been shown that at least one higher frequency components of the tide, the terdiurnal tide, can at times be of the same magnitude, and even larger, than the semidiurnal tide. By understanding when and why this happens this information can be included in current models for the atmospheric tidal oscillations.



## Chapter 2

# Atmospheric tidal waves

This chapter is based on [1],[2],[3], [4], [5], [6], [7] and [8].

Tidal oscillations are a well known thermally driven phenomenon observed in the atmosphere. During the day there is heating of the atmosphere by the absorption by  $H_2O$  and  $O_3$ , however there is no heating when the sun is down. When the atmosphere is heated, it expands which causes a pressure gradient and a forcing of the wind. This on/off nature of the atmospheric heating means this forcing cannot be explained by a single sinusoidal wave, and must instead be described by a Fourier series. The components of this Fourier series are what we can observe as the tidal oscillations in the atmospheric wind. Mathematically the heating can be described by the following equation, as it also depends on the altitude and latitude:

$$J_\lambda(t) = \sum_n A_n(z, \theta, \lambda) \cos\left(\frac{n2\pi t}{24}\right) + \phi_n(z, \theta)$$

where different values of  $n$  separate the different components. These are called diurnal ( $n = 1$ ), semidiurnal ( $n = 2$ ), terdiurnal ( $n = 3$ ), quaterdiurnal ( $n = 4$ ) and so on.

There are two types of atmospheric tidal waves, migrating and non-migrating waves. The migrating waves are the ones that follow the sun around, and can be observed at different times in different parts of the world. Over certain types of land however, a wave that is non-migrating may be observed. This is a kind of tidal oscillation that depend on longitude as well as local time. The non-migrating tide is in general not the dominant part, unless the altitude of interest is below 30 km. Below that altitude the non-migrating tide may be dominant.

The latitudinal dependence of the tidal waves is the solution of Laplace's tidal equations[1]. This solution consists of an infinite number of eigenfunctions called Hough functions and their associated eigenvalues or separation constants. By expanding the forcing in terms of these Hough functions one can find the response to the forcing by each eigenfunction, also referred to as equivalent depth. For the migrating semidiurnal tide, the Hough functions are similar to the La-

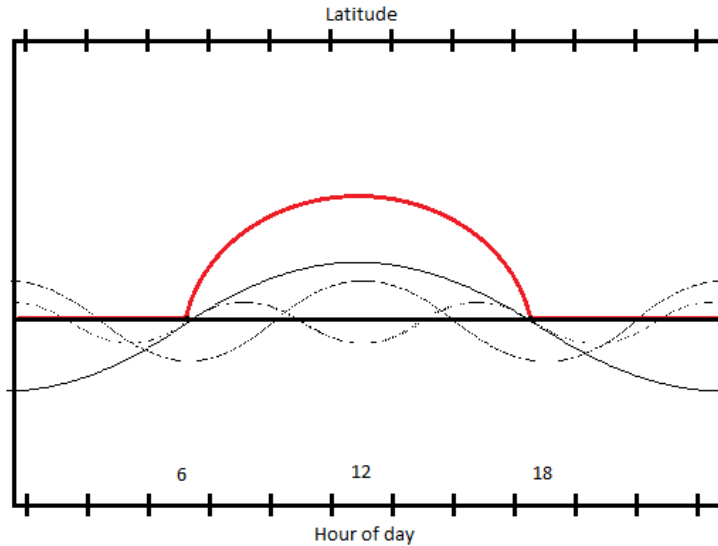


Figure 2.1: Illustration of the different Fourier components of the wind (black) that are produced by the heating (red)

large polynomials of order two. All the Hough functions for the semidiurnal tide have positive equivalent depths. For the migrating diurnal tide there are two dominating sets of Hough functions. One with relatively small positive depths which is restricted to the equatorial side of  $\theta = 30^\circ$ . The other set has negative equivalent depths and is situated pole-wards from  $\theta = 30^\circ$ . The reason for this limit is that pole-wards from  $\theta = 30^\circ$  the Coriolis parameter exceeds the frequency of the diurnal tide. Because of this we can see the situation that the semidiurnal tide is more dominant than the diurnal tide at some latitudes. The semidiurnal is generally the dominant tidal wave over Dragvoll, which is where the radar used for observations in this project is situated.

The theory on the terdiurnal tidal component is that it exists due to non-linear interactions between the diurnal and the semidiurnal wave. One would expect that the amplitude of the terdiurnal tide is small compared to the diurnal and semidiurnal tide, however some papers ([8], [7]) have previously shown that it may at times have amplitudes comparable to the one of the diurnal and semidiurnal.

The quaterdiurnal tide is another higher order mode of the tides with a frequency of 6 hours.



## Chapter 3

# The SKiYMET meteor radar

This chapter is based on information from [9] and [10].

The data upon which this project is based comes from a SKiYMET radar located at Dragvoll, Trondheim. This piece of equipment utilizes eight transmitter antennas and five receiver antennas and receives information about ionized trails left behind by meteors entering the atmosphere. These trails last for up to about four seconds as they burn up in the atmosphere, and during this time they will drift with the wind. The information includes the line of sight velocity of the trail, distance from the radar, azimuth angle, zenith angle and ambiguity. Due to the high number of transmitter and receiver antennas the SKiYMET radar can detect meteors in a great span of zenith angle, and it can receive data from many more meteors each day, compared to older types of radars. This gives more possibilities when it comes to treating this information. The transmitting antennas transmit at a frequency of about 1 kHz, while the receiving antennas sample at a frequency of 34.21 MHz, and wavelength  $\lambda \approx 9m$ . The eight transmitting antennas are placed in an octagon with about  $1\lambda$  of distance to nearest neighbor. This setup is to focus the radiation towards zenith angle  $10^\circ - 90^\circ$ , and ignore the area around zenith. This setup also causes destructive interference for some azimuth angles, at multiples of  $45^\circ$ , while it has positive interference between these angles.

The receiving antennas are set up as a cross with one antenna in the middle, and the four placed around it with  $90^\circ$  between them (as in figure ??). Two of the antennas are placed at a distance of  $r = 2\lambda$  away from the middle antenna, while the two others are placed at a distance of  $r = \lambda$ .

Using this setup, the difference in phase at the different antennas makes it possible to determine the position of the detected meteor. This is done by predicting several positions where the meteor can have been detected, and choosing

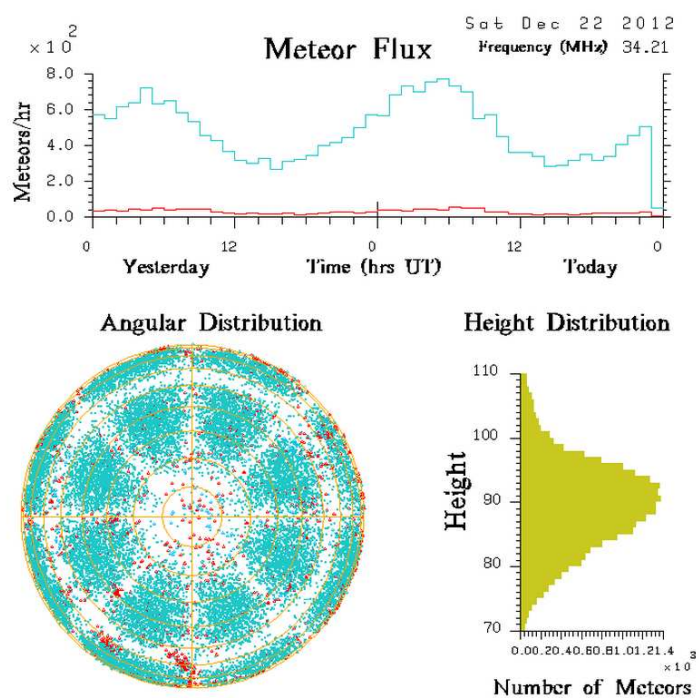


Figure 3.1: Example of the meteor distribution. Picture from the atmospheric groups webpage [11]

the one which gives the lowest error, given that the error is smaller than a given threshold. If two or more positions give the lowest error, the meteor is marked as ambiguous and the number of ambiguous points is noted in the output file. The number of meteors detected by the radar varies from day to day and also within the day, with an average of about 15,000 detections a day. This meteor flux varies through the day, since the earth rotates around itself as well as around the sun and it is usually highest when the radar sees along the earth's orbit around the sun. This means that the tilt of the earth relative to the earth's orbit will affect the number of meteors we can detect. For this reason we can expect to detect more meteors in the summer half of the year, than what we can expect during the winter.



Figure 3.2: Overview picture of the setup of the SKiYMET radar at Dragvoll. Picture from [9]

```

1 Version 2.2
2 SITENAME trondheim
3 LOCATION +63.4,+10.5
4 TIME_ZONE 1.000000
5 FREQUENCY(MHz) 34.210
6 LO_FREQUENCY(MHz) 44.910
7 CHANNELS 10
8 RESOLUTION(KM) 2.0
9 GATES 30
10 START_RGE(KM) 4.0
11 PRF 2144
12 ANTENNA_COORDS 17.53 14.00 21.84 194.00 21.94 104.00 17.54 284.00 .00 .00
13 PHASE_OFFSETS .00 25.60 58.20 66.90 45.40
14 INTEGRATIONS 4
15 RECORD_LENGTH 4.00
16 NSMOOTH 5
17 MINHT 70
18 MAXHT 110
19 RXLIST 1 1 1 1 1
20 RX_GAIN 1107
21 TIME_ACCURACY HIGH
22 GPS_STATUS LOCK 63.406811 N 10.467659 E
23 VEL_ERR_LIM 5.50
24 SN_ACCEPT_RATIO 2.00
25 T_DECAY_MAX 2.00
26 PLANE_NORMAL 1.72 104.00
27 PULSE_CODE 1
28 MODE I
29 Date Time File Rge Ht Vrad delVr Theta Phi0 Ambig Delphase ant pair IREX amax Tau vmet snrdb
30 2012/08/14 0:00:09.048 00000 171.9 99.9 51.71 1.87 55.1 223.6 1 19.6 45 1 33309. .025 -9.99 30.5
31 2012/08/14 0:00:09.035 00001 169.9 98.2 57.37 .12 55.3 223.5 1 12.4 54 1 10764. .035 -9.99 20.8
32 2012/08/14 0:00:08.826 00002 157.9 87.5 -11.31 3.64 56.9 203.4 3 34.3 35 1 1822. .095 -9.99 6.1
33 2012/08/14 0:00:08.826 00002 367.8 79.6 -11.31 3.64 79.1 242.3 3 32.2 51 1 1822. .095 -9.99 6.1
34 2012/08/14 0:00:08.826 00002 437.8 97.0 -11.31 3.64 79.1 242.3 3 32.2 51 1 1822. .095 -9.99 6.1
35 2012/08/14 0:00:10.166 00003 112.0 94.8 -38.17 .28 32.4 117.3 1 15.3 52 1 12873. .026 -9.99 21.4
36 2012/08/14 0:00:10.166 00004 114.0 96.6 -38.55 .38 32.3 117.2 1 16.4 25 1 9041. .025 -9.99 18.8
37 2012/08/14 0:00:13.541 00006 118.0 98.4 12.36 .79 33.7 10.4 2 25.6 54 1 3340. .122 -9.99 10.4
38 2012/08/14 0:00:13.541 00006 118.0 87.3 12.36 .79 42.6 71.0 2 16.9 25 1 3340. .122 -9.99 10.4
39 2012/08/14 0:00:13.543 00007 116.0 96.9 13.33 1.46 33.6 9.8 2 25.8 15 1 2553. .123 -9.99 8.4
40 2012/08/14 0:00:13.543 00007 116.0 86.4 13.33 1.46 42.2 70.9 2 17.5 52 1 2553. .123 -9.99 8.4
41 2012/08/14 0:00:25.261 00008 100.0 93.1 -6.99 .64 21.5 163.6 1 16.6 35 1 7808. .039 -9.99 17.8
42 2012/08/14 0:00:35.897 0000A 159.9 91.0 49.96 .62 55.9 322.8 1 14.6 45 1 4683. .148 -9.99 13.1
43 2012/08/14 0:00:36.056 0000C 106.0 105.1 1.77 3.36 7.2 348.1 2 27.4 51 1 2001. .033 -9.99 6.0
44 2012/08/14 0:00:36.056 0000C 106.0 88.5 1.77 3.36 33.7 111.7 2 29.9 35 1 2001. .033 -9.99 6.0
45 2012/08/14 0:00:36.838 0000D 233.9 90.0 -55.34 1.74 68.3 160.6 2 24.8 25 1 6389. .049 -9.99 15.6
46 2012/08/14 0:00:36.838 0000D 94.0 76.2 -55.34 1.74 36.1 203.4 2 21.5 45 1 6389. .049 -9.99 15.6
47 2012/08/14 0:00:36.840 0000E 231.9 90.9 -58.19 .41 67.9 160.7 2 20.1 52 1 8219. .050 -9.99 16.6
48 2012/08/14 0:00:36.840 0000E 92.0 74.6 -58.19 .41 36.0 203.7 2 26.8 45 1 8219. .050 -9.99 16.6
49 2012/08/14 0:00:41.203 0000G 169.9 93.0 -20.71 2.92 57.5 152.9 2 29.9 45 1 3843. .032 -9.99 11.5

```

Figure 3.3: Example of output file from the SKiYMET meteor radar. Data used in this project: Time, Ht: Height, Vrad: Line of sight velocity, Theta: zenith angle, Phi0: Azimuth angle, ambig: ambiguity level

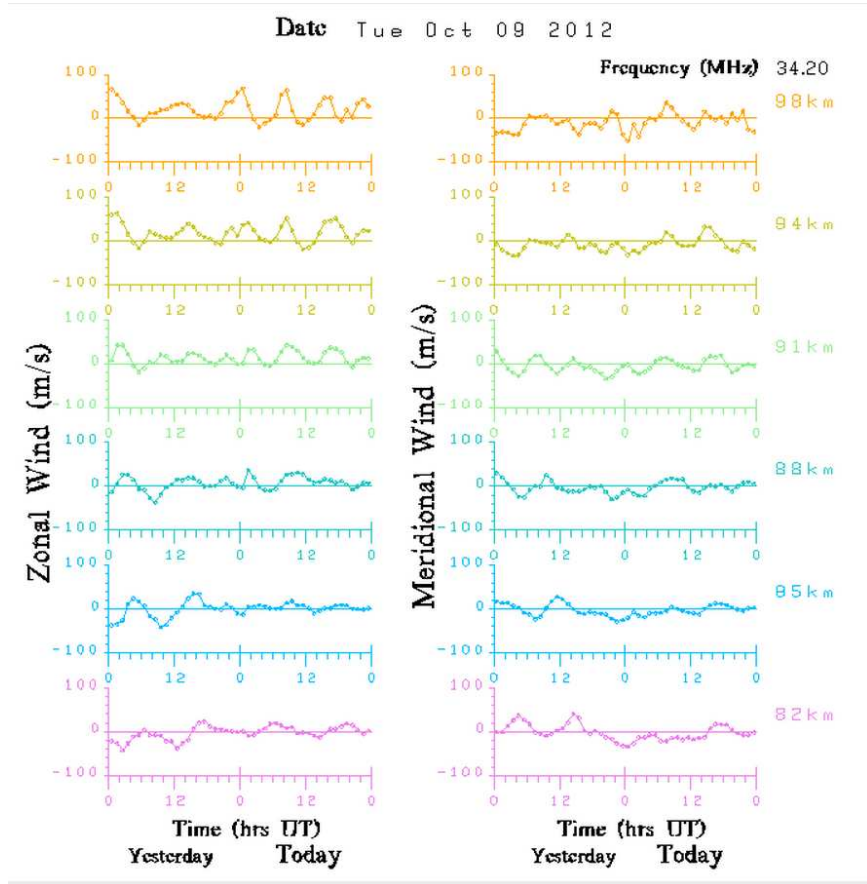


Figure 3.4: Example of the graphic of the zonal and meridional wind that can be found at the atmospheric groups homepage [11]



# Chapter 4

## Method

To find the tidal components from the wind measurements, the first thing that had to be done was to find the winds. This was done by assuming no vertical component of the wind and fit, using a least square routine in Matlab, a U (zonal) and V (meridional) component to the equation:  $V_{LOS} = U \cdot \cos(\theta)\cos(\phi) + V \cdot \sin(\theta)\sin(\phi)$

Here  $V_{LOS}$  are the line of sight velocities,  $\theta$  are the zenith angles and  $\phi$  are the azimuth angles of meteors detected in the desired height and time. The sorting in time and height was set to one hour of data and 76k-81km, 81-84km, 84-87km, 87-90km, 90-93km, 93-96km, 96-99km and 99-104km. As the stream of meteors in all altitudes is not constant, there would not be fitted any U or V component if there was less then 3 meteors at the desired altitude at a given time. The error found from this fit would be used as weighting in the later fits in the routine given by:

$$weight = \frac{1}{\sigma^2}$$

These U and V values are stored in datasets of 7 days at a time, in order to investigate 6 days of data with the entire day it is fitting tides to in the middle of the dataset. These are later in the code saved to a textfile so that they can be analyzed at a later time without going through the whole sorting and fitting process.

When trying to find the tidal components of the data from the meteor radar, the first approach was to fit all components at once to a four day set of the data. This method would find some amplitudes and phases, however there was some concern about the higher frequency components. If the six/eight hour tidal waves were to have a spike of the amplitude over a couple of days, this might not be seen in the data with this approach. A decision was therefore made to fit each component over  $3\lambda$  of that components (six days for a 48-hour, three days for the diurnal and so on.). This was implemented by fitting the 48-hour to six days, subtracting it from the data, narrow down to three days, fit the diurnal, subtract that, and so on. This was done down to 18 hours a 6-hour component, and the phase, amplitude and error of each fit was subtracted. The 12 and 24 hour as well as a constant was also included in the 48 hour fit and the

12 hour was included in the diurnal fit. This was done in order to ensure that the error of these fits would be as accurate as possible, as the 48-hour alone is not a good fit of data that consists mainly of a semidiurnal component. When the semidiurnal was fitted, the constant from that fit was also subtracted from the data. The terdiurnal and quaterdiurnal was then fitted to the data, with no other components in the fitting routine. For all the fitting routines, the fitted component would not be removed from the data if the amplitude was found to be insignificant, i.e. if the amplitude was smaller than  $1\sigma$ .

# Chapter 5

## Results

The following figures contain the results gotten from running the Matlab-routine on data from September 10th to April 30th. They are represented with contour diagrams and a corresponding color axis to give the magnitude of the different points. Times and heights where no significant amplitude could be found are represented by the blacked out areas which can be found in all the plots. Significant values are values greater than  $1\sigma$  and with more than  $\frac{2}{3}$  of the points in the dataset present. All the plots has a greater lack of data in the 99-104 km range then for the other altitudes, so this altitude has more blacked out areas then the others.

Figure 5.1 shows the significant amplitudes found for the diurnal wave. Compared to figure 5.3 the amplitudes of the diurnal wave is generally smaller then the ones for the semidiurnal, which is expected at these latitudes. The zonal part of the diurnal looks to have a spike in the magnitude of the amplitudes around the early part/middle of January.

In the datasets for the semidiurnal amplitude two values were removed in order to make the contour plot practical to look at and understand. One amplitude in the zonal part of the semidiurnal was found to be 1,477 m/s, which made the rest of the plot have the same color. In the meridional part of the semidiurnal an amplitude of 325 m/s was found which had the same impact.

For the terdiurnal component there was found significant amplitudes in 62.7% and 64.9% for the zonal and meridional parts. The altitude with the lowest percentage was 99-104 km, with 40.3% and 46.4% for U and V. At the other altitudes the amount of of significant data ranged from 58.4% – 74.7%. The monthly and annual averages of these can be found in tables 5.1-5.4.

On a few occasions the value of the terdiurnal wave was found to be up to  $70m/s$  for the meridional and  $65\frac{m}{s}$  for the zonal, however these points also have  $2\sigma$ -values which are close to or higher then the amplitude. An exception is October 20th, where the value for the amplitude was found to be  $54.9\frac{m}{s}$ , while  $2\sigma = 51.4\frac{m}{s}$ , which is a small value for  $\sigma$  compared to the other high value

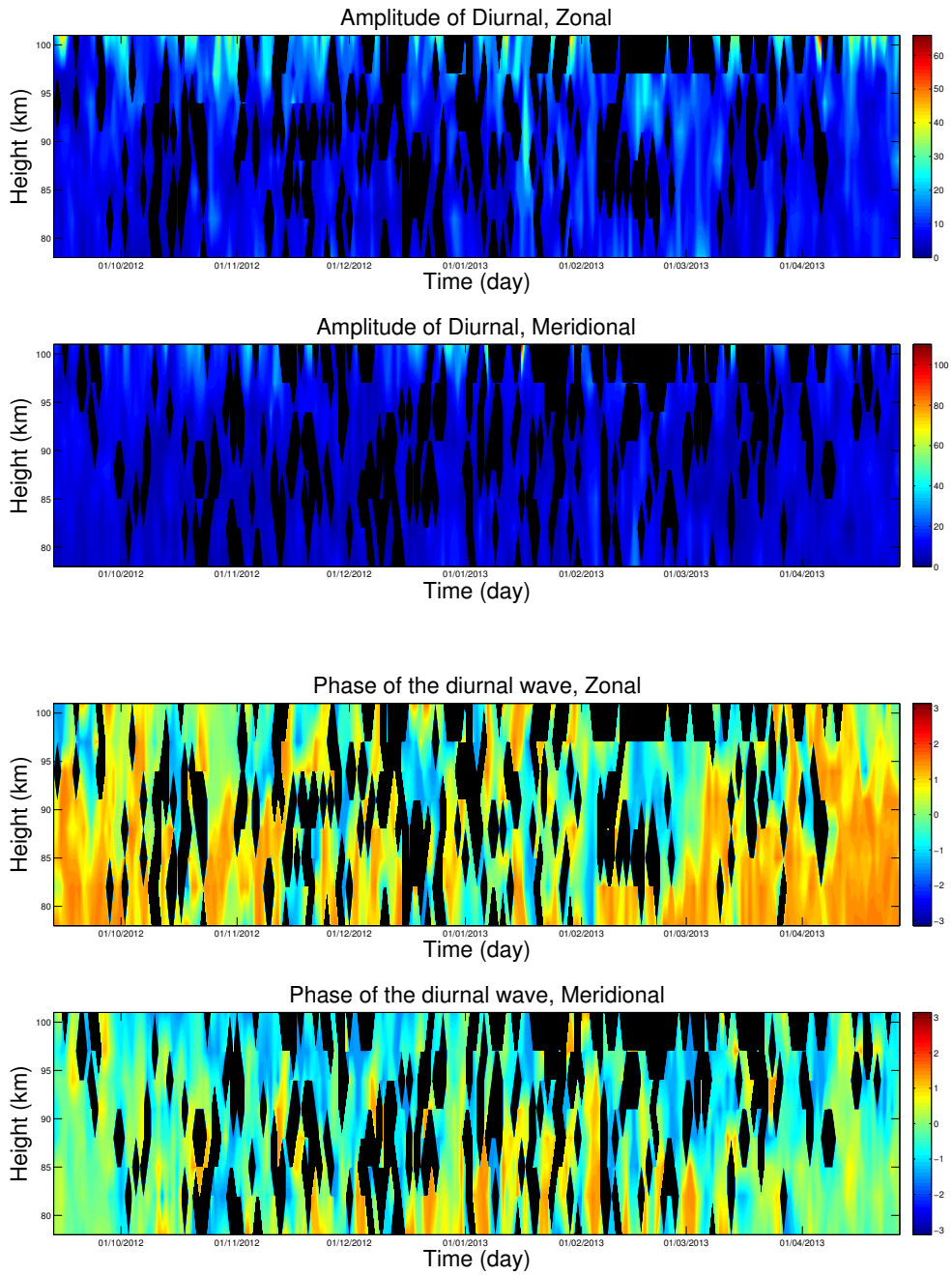


Figure 5.1: (a) Significant amplitudes for the diurnal wave from the period September 10th to April 30th. (b)  $2\sigma$  error of the amplitudes.

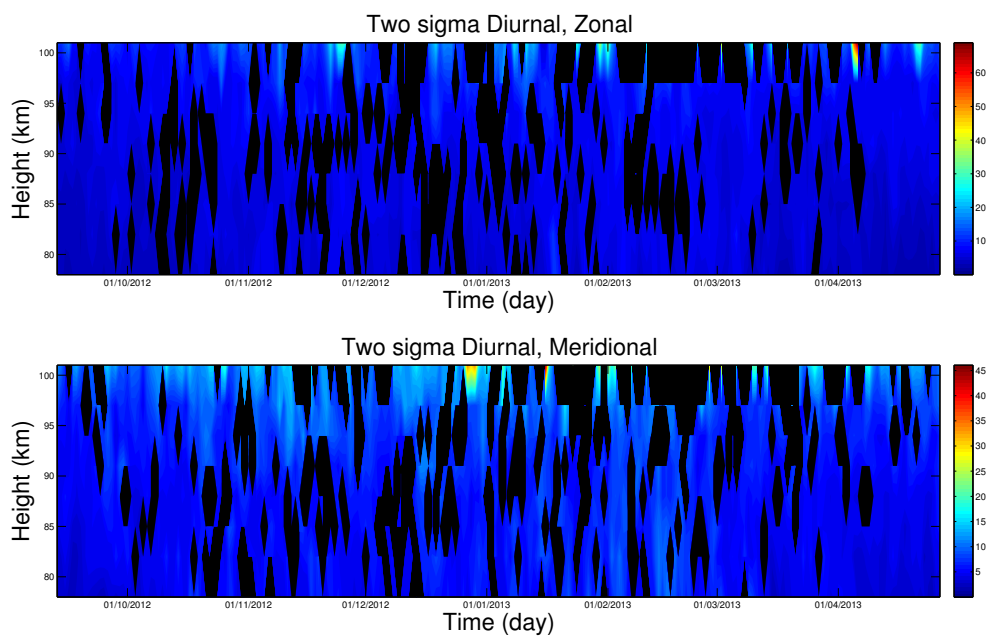


Figure 5.2: Corresponding  $2\sigma$  to the amplitudes of the diurnal in figure5.1

Table 5.1: Overall means of the significant amplitudes found of the zonal component. The numbers inside the brackets are the mean calculated without the values removed from the plot.

Altitude (km)	48-hour (m/s)	24-hour (m/s)	12-hour (m/s)	8-hour (m/s)	6-hour (m/s)
76 – 81	$5.6 \pm 3.4$	$7.8 \pm 3.7$	$15.1 \pm 7.3$	$9.1 \pm 3.3$	$7.6 \pm 3.8$
81 – 84	$5.6 \pm 2.9$	$7.6 \pm 3.1$	$18.6 \pm 9.2$	$11.7 \pm 4.9$	$8.3 \pm 3.9$
84 – 87	$5.8 \pm 2.7$	$7.3 \pm 3.2$	$20.2 \pm 10.9$	$12.0 \pm 5.1$	$8.7 \pm 4.1$
87 – 90	$5.6 \pm 2.4$	$8.1 \pm 3.9$	$24.1 \pm 12.1$	$12.5 \pm 5.7$	$9.5 \pm 4.7$
90 – 93	$5.7 \pm 2.2$	$8.7 \pm 4.3$	$28.4 \pm 14.3$	$14.0 \pm 6.2$	$9.8 \pm 4.4$
93 – 96	$6.5 \pm 3.0$	$10.2 \pm 4.7$	$35.2 \pm 17.3$	$15.5 \pm 6.9$	$11.1 \pm 5.0$
96 – 99	$7.9 \pm 4.1$	$12.6 \pm 5.8$	$39.6 \pm 18.6$	$17.8 \pm 7.3$	$13.0 \pm 5.7$
99 – 104	$21.5 \pm 57.9$	$22.1 \pm 10.8$	$49.6 \pm 108.9$ ( $41.7 \pm 20.1$ )	$25.9 \pm 9.9$	$22.8 \pm 12.6$

points for the amplitude. The amplitudes for the terdiurnal does also tend to have the highest values for the amplitudes at the highest altitudes, which is consistent with what can be seen for the semidiurnal.

For the quaterdiurnal wave there was found significant values of the amplitude in 70.7% of the dataset (73.0% for U, 69.4% for V). As for the terdiurnal the 99-104km range was the one with the fewest significant values (54.0% and 51.0%), while the others ranged from 66.5% to 82.4%. In the plot of the the six-hour quaterdiurnal wave a value in the meridional plot was removed. The reason for this is the same as for the semidiurnal amplitudes. The value was found to be 2149 m/s, and occurred on the 21st of January.

One value was removed from the plot of the background wind in figure 5.9, because it had a high value while having an error too great for it to be significant. This was done for the Zonal part on 9. February 2012. It is worth to note that the 2sigma value on the dates 5. December 2012 (U), 31. March (U and V) and 32. march (V). Have extremely high  $2\sigma$  values. These were not removed because the values themselves are of the same order as surrounding points in the figure. As this project's main focus is on the oscillations rather than the background wind, all the points except the one is included in the plot regardless of whether the value was significant in order to see the overall changes of the background wind.

Table 5.2: Overall means of the significant amplitudes found of the meridional component. The numbers inside brackets are means calculated without the values that were removed from the plot.

Altitude (km)	48-hour (m/s)	24-hour (m/s)	12-hour (m/s)	8-hour (m/s)	6-hour (m/s)
76 – 81	$6.7 \pm 3.9$	$8.6 \pm 4.0$	$15.8 \pm 7.2$	$10.1 \pm 4.4$	$7.7 \pm 3.9$
81 – 84	$9.5 \pm 23.6$	$8.4 \pm 3.8$	$18.9 \pm 9.5$	$11.5 \pm 4.7$	$8.3 \pm 4.0$
84 – 87	$6.1 \pm 2.8$	$7.8 \pm 3.4$	$21.3 \pm 11.1$	$12.0 \pm 5.1$	$8.7 \pm 4.3$
87 – 90	$5.6 \pm 2.1$	$8.2 \pm 3.5$	$24.4 \pm 12.1$	$12.7 \pm 5.2$	$8.8 \pm 4.3$
90 – 93	$6.4 \pm 2.4$	$8.2 \pm 3.0$	$28.7 \pm 13.7$	$14.2 \pm 5.9$	$9.8 \pm 4.5$
93 – 96	$6.6 \pm 3.4$	$9.4 \pm 3.8$	$35.0 \pm 16.3$	$15.4 \pm 6.8$	$10.7 \pm 5.4$
96 – 99	$8.7 \pm 5.2$	$12.7 \pm 5.7$	$39.2 \pm 17.4$	$18.2 \pm 8.2$	$12.7 \pm 5.8$
99 – 104	$19.6 \pm 21.9$	$23.6 \pm 13.0$	$44.2 \pm 30.8$ ( $41.7 \pm 20.5$ )	$26.0 \pm 11.6$	$45.7 \pm 196.1$ ( $28.0 \pm 30.1$ )

Table 5.3: Monthly means for the zonal part of the terdiurnal wave. (2012-2013)

Altitude (km)	September (m/s)	October (m/s)	November (m/s)	December (m/s)	January (m/s)	February (m/s)	March (m/s)	April (m/s)
76-81	$6.7 \pm 2.4$	$8.7 \pm 3.2$	$10.7 \pm 3.0$	$9.9 \pm 3.4$	$10.1 \pm 3.4$	$10.3 \pm 2.3$	$9.0 \pm 4.3$	$7.9 \pm 2.6$
81-84	$11.0 \pm 5.2$	$12.1 \pm 5.1$	$13.0 \pm 4.8$	$11.0 \pm 3.8$	$12.1 \pm 5.3$	$15.5 \pm 5.1$	$10.6 \pm 4.3$	$8.5 \pm 2.7$
84-87	$10.7 \pm 5.1$	$12.7 \pm 4.5$	$14.1 \pm 5.6$	$12.9 \pm 4.4$	$11.0 \pm 5.4$	$15.0 \pm 5.4$	$11.3 \pm 4.9$	$8.7 \pm 3.1$
87-90	$11.7 \pm 4.9$	$11.3 \pm 4.7$	$14.7 \pm 5.7$	$13.7 \pm 4.7$	$13.9 \pm 5.0$	$15.2 \pm 5.6$	$10.0 \pm 3.8$	$11.0 \pm 4.7$
90-93	$12.6 \pm 5.0$	$12.3 \pm 6.1$	$13.5 \pm 4.1$	$17.3 \pm 7.4$	$14.2 \pm 5.9$	$15.5 \pm 6.9$	$11.5 \pm 6.2$	$14.4 \pm 5.3$
93-96	$13.8 \pm 8.3$	$14.1 \pm 5.7$	$15.8 \pm 5.2$	$22.1 \pm 8.3$	$13.8 \pm 4.7$	$14.9 \pm 7.8$	$13.0 \pm 5.8$	$15.9 \pm 5.4$
96-99	$11.0 \pm 5.1$	$16.5 \pm 8.2$	$20.8 \pm 7.2$	$20.9 \pm 8.4$	$16.8 \pm 6.2$	$18.9 \pm 6.6$	$17.3 \pm 5.7$	$17.4 \pm 5.8$
99-104	$23.3 \pm 5.3$	$21.8 \pm 7.5$	$29.7 \pm 8.9$	$26.5 \pm 9.8$	$28.3 \pm 13.9$	$33.4 \pm 16.0$	$16.6 \pm 10.6$	$22.5 \pm 9.5$

Table 5.4: Monthly means for the meridional part of the terdiurnal wave. (2012-2013)

Altitude (km)	September (m/s)	October (m/s)	November (m/s)	December (m/s)	January (m/s)	February (m/s)	March (m/s)	April (m/s)
76-81	$5.56 \pm 2.5$	$11.3 \pm 5.4$	$10.0 \pm 4.4$	$10.7 \pm 3.8$	$10.8 \pm 4.5$	$13.0 \pm 2.9$	$10.3 \pm 4.4$	$7.6 \pm 2.3$
81-84	$10.2 \pm 4.7$	$11.3 \pm 4.8$	$12.0 \pm 5.5$	$11.9 \pm 3.8$	$10.9 \pm 4.0$	$15.0 \pm 5.0$	$11.4 \pm 4.8$	$9.0 \pm 3.1$
84-87	$11.6 \pm 6.4$	$11.1 \pm 4.0$	$12.9 \pm 5.0$	$14.2 \pm 3.6$	$12.2 \pm 5.6$	$15.0 \pm 6.1$	$11.7 \pm 5.4$	$8.5 \pm 3.1$
87-90	$12.7 \pm 5.9$	$10.1 \pm 3.9$	$12.4 \pm 4.7$	$12.9 \pm 5.0$	$14.8 \pm 6.9$	$16.3 \pm 5.5$	$11.8 \pm 4.2$	$11.0 \pm 3.9$
90-93	$11.6 \pm 6.2$	$12.9 \pm 5.2$	$16.0 \pm 4.6$	$17.3 \pm 7.6$	$13.2 \pm 5.9$	$15.7 \pm 7.0$	$13.0 \pm 3.3$	$12.7 \pm 4.5$
93-96	$11.8 \pm 5.4$	$14.3 \pm 4.7$	$15.8 \pm 6.6$	$17.7 \pm 6.5$	$16.1 \pm 9.8$	$17.4 \pm 7.5$	$14.4 \pm 5.2$	$13.2 \pm 6.5$
96-99	$13.9 \pm 4.9$	$14.8 \pm 6.3$	$19.5 \pm 5.7$	$19.7 \pm 6.1$	$20.1 \pm 14.5$	$20.4 \pm 5.4$	$17.6 \pm 6.8$	$17.8 \pm 8.8$
99-104	$18.4 \pm 8.8$	$23.3 \pm 10.5$	$26.2 \pm 10.0$	$28.7 \pm 11.1$	$30.1 \pm 17.8$	$34.7 \pm 10.2$	$27.8 \pm 11.0$	$25.8 \pm 11.2$

Table 5.5: Monthly means for the zonal part of the quaterdiurnal wave. (2012-2013)

Altitude (km)	September (m/s)	October (m/s)	November (m/s)	December (m/s)	January (m/s)	February (m/s)	March (m/s)	April (m/s)
76-81	$4.7 \pm 1.7$	$6.8 \pm 2.0$	$10.1 \pm 4.4$	$7.5 \pm 3.1$	$8.5 \pm 4.2$	$9.9 \pm 4.1$	$6.6 \pm 3.2$	$4.8 \pm 2.3$
81-84	$4.8 \pm 1.5$	$8.1 \pm 3.4$	$11.0 \pm 3.9$	$8.2 \pm 3.2$	$7.0 \pm 2.8$	$10.5 \pm 4.7$	$8.2 \pm 4.3$	$6.1 \pm 2.3$
84-87	$6.4 \pm 3.6$	$7.9 \pm 3.2$	$10.0 \pm 4.8$	$9.5 \pm 4.6$	$7.9 \pm 3.2$	$12.2 \pm 4.3$	$8.5 \pm 3.7$	$6.7 \pm 2.0$
87-90	$6.6 \pm 2.5$	$8.7 \pm 4.3$	$11.7 \pm 4.4$	$11.8 \pm 5.9$	$9.2 \pm 3.8$	$11.4 \pm 4.5$	$8.3 \pm 4.3$	$8.3 \pm 4.7$
90-93	$8.6 \pm 3.5$	$9.5 \pm 5.0$	$10.8 \pm 4.7$	$10.5 \pm 5.2$	$9.9 \pm 3.8$	$10.1 \pm 3.6$	$9.1 \pm 5.0$	$9.2 \pm 3.8$
93-96	$8.8 \pm 3.7$	$10.2 \pm 4.0$	$13.0 \pm 5.8$	$12.3 \pm 5.7$	$12.0 \pm 5.0$	$10.4 \pm 5.5$	$10.4 \pm 4.9$	$11.1 \pm 4.5$
96-99	$7.0 \pm 2.8$	$11.1 \pm 4.4$	$14.5 \pm 5.0$	$13.5 \pm 4.8$	$16.2 \pm 9.7$	$13.1 \pm 3.9$	$13.8 \pm 4.3$	$12.0 \pm 3.5$
99-104	$11.9 \pm 5.8$	$14.4 \pm 5.3$	$26.3 \pm 12.0$	$24.0 \pm 14.0$	$29.3 \pm 14.0$	$35.3 \pm 14.2$	$22.7 \pm 12.2$	$22, 7 \pm 11.3$

Table 5.6: Monthly means for the meridional part of the quaterdiurnal wave. (2012-2013)

Altitude (km)	September (m/s)	October (m/s)	November (m/s)	December (m/s)	January (m/s)	February (m/s)	March (m/s)	April (m/s)
76-81	$5.4 \pm 1.8$	$7.9 \pm 4.4$	$8.3 \pm 3.4$	$9.1 \pm 4.9$	$7.6 \pm 3.2$	$10.7 \pm 3.8$	$6.7 \pm 3.0$	$5.0 \pm 2.5$
81-84	$5.5 \pm 1.7$	$8.2 \pm 4.3$	$8.6 \pm 2.9$	$9.3 \pm 3.4$	$9.1 \pm 2.8$	$13.2 \pm 5.8$	$6.9 \pm 3.0$	$6.0 \pm 3.2$
84-87	$6.9 \pm 4.0$	$7.9 \pm 4.4$	$10.5 \pm 4.9$	$9.4 \pm 3.4$	$8.3 \pm 3.4$	$11.3 \pm 5.5$	$8.6 \pm 3.2$	$5.8 \pm 3.0$
87-90	$6.9 \pm 3.5$	$9.0 \pm 5.5$	$8.7 \pm 3.9$	$10.0 \pm 4.7$	$8.7 \pm 3.9$	$11.0 \pm 4.9$	$8.3 \pm 3.3$	$7.3 \pm 2.9$
90-93	$7.5 \pm 3.7$	$9.2 \pm 4.9$	$11.1 \pm 5.4$	$11.7 \pm 4.5$	$9.4 \pm 4.0$	$11.9 \pm 3.6$	$8.3 \pm 3.5$	$8.2 \pm 3.8$
93-96	$8.4 \pm 3.8$	$10.0 \pm 5.4$	$14.1 \pm 7.1$	$10.6 \pm 4.5$	$10.5 \pm 5.2$	$13.3 \pm 5.0$	$10.5 \pm 5.8$	$8.2 \pm 3.5$
96-99	$10.3 \pm 4.1$	$11.7 \pm 5.9$	$15.5 \pm 6.2$	$14.0 \pm 4.7$	$14.4 \pm 7.4$	$14.3 \pm 6.1$	$12.4 \pm 5.1$	$9.2 \pm 3.1$
99-104	$14.7 \pm 7.5$	$20.8 \pm 9.5$	$22.1 \pm 9.6$	$40.1 \pm 52.2$	$173.5 \pm 529.2$ ( $41.7 \pm 50.4$ )	$41.8 \pm 17.9$	$25.6 \pm 12.2$	$21.6 \pm 9.6$

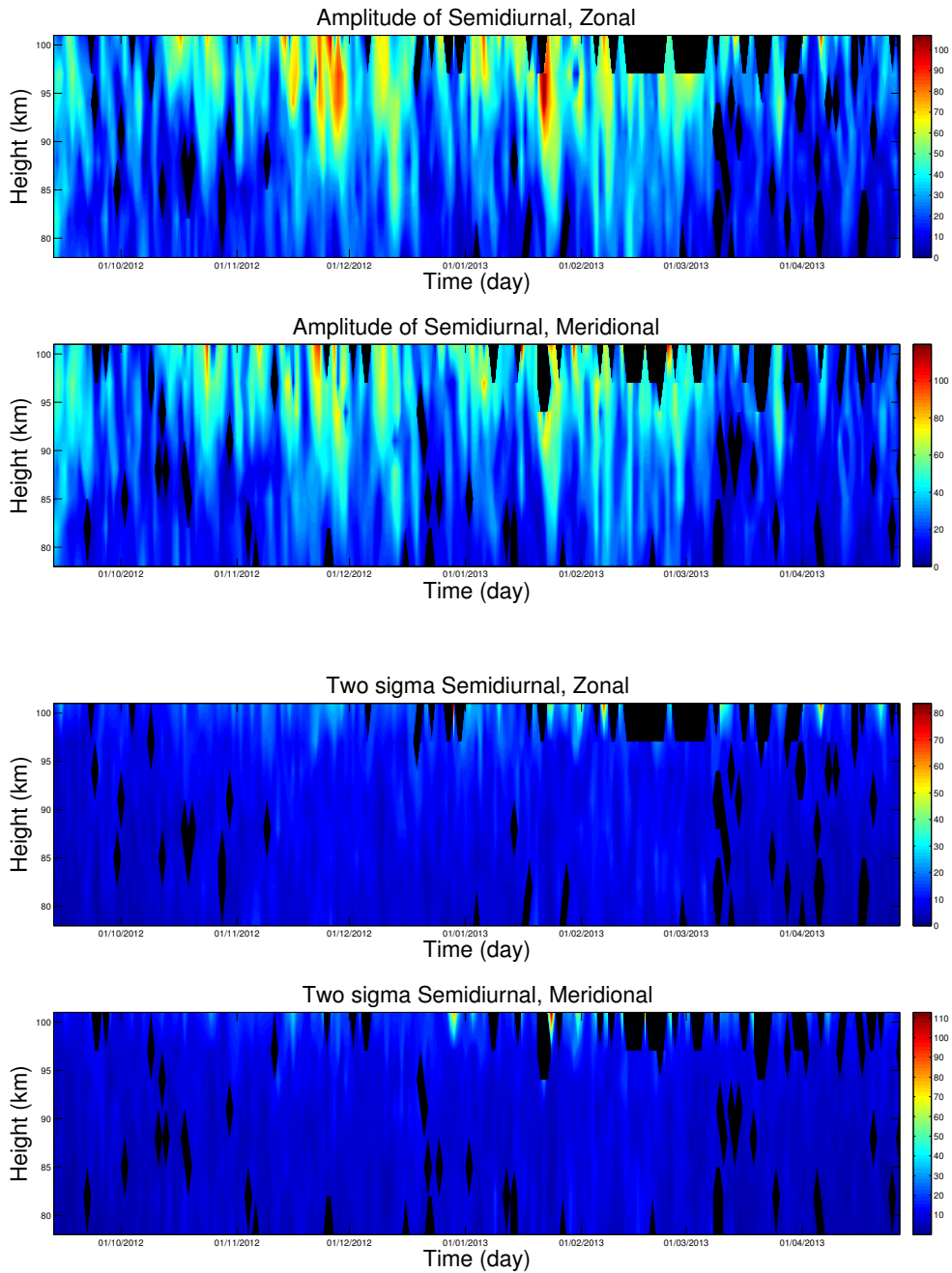


Figure 5.3: (a) Significant amplitudes found for the semidiurnal tidal wave in the period from September 10th 2012 until April 30th 2013. (b)  $2\sigma$  error of the amplitudes.

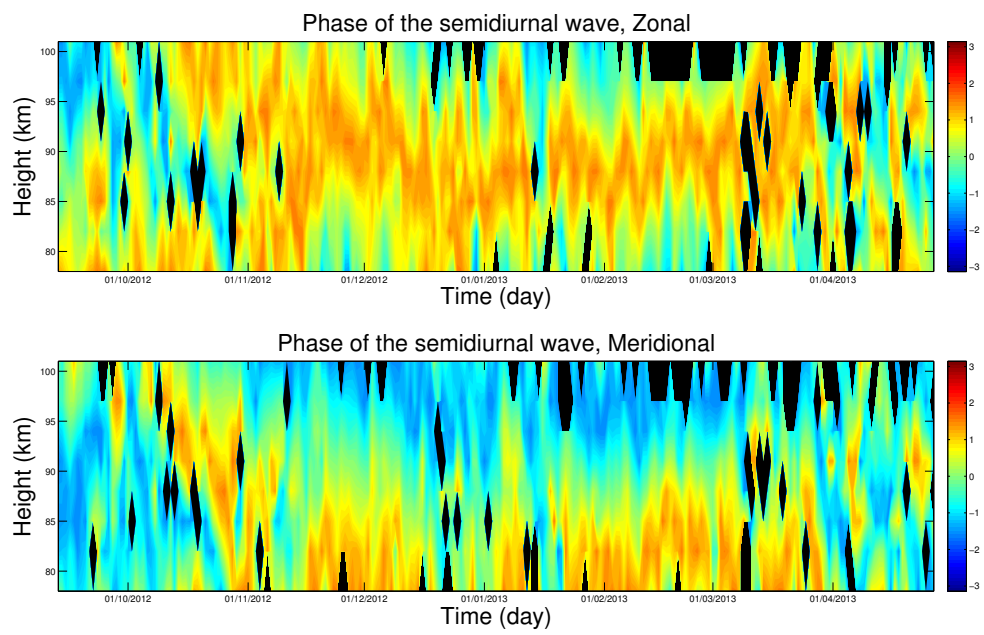


Figure 5.4: Corresponding phases to the amplitudes of the semidiurnal in figure 5.3.

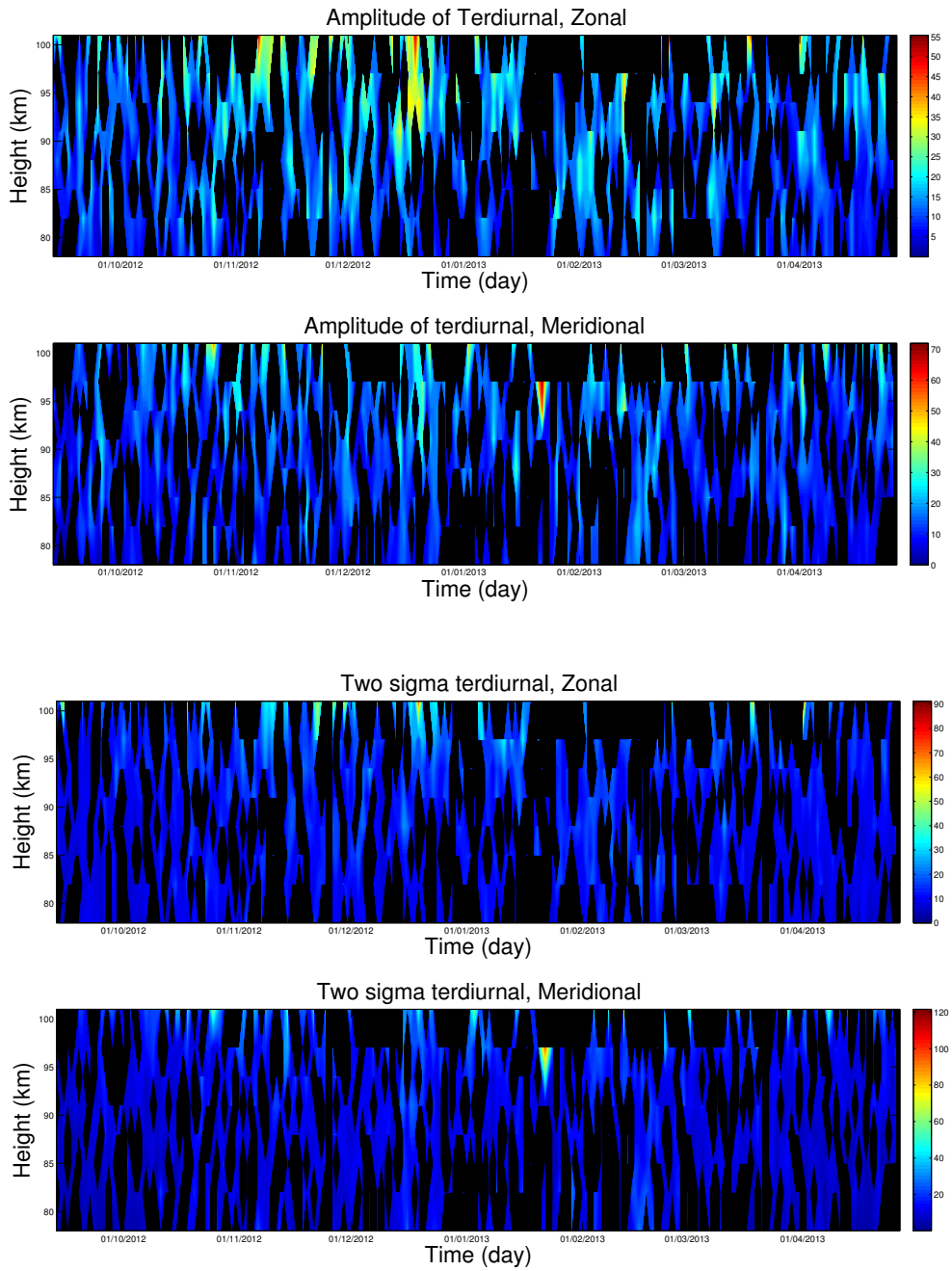


Figure 5.5: (a) Significant amplitudes found for the terdiurnal tidal wave in the period September 10th 2012 until April 30th 2013. (b) corresponding  $2\sigma$  error.

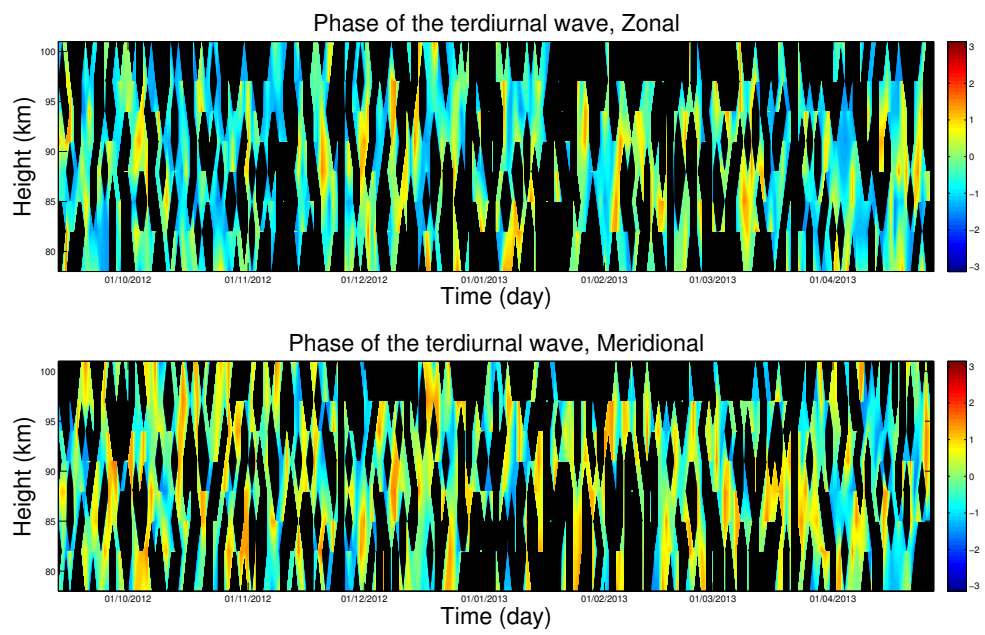


Figure 5.6: Corresponding phases to the amplitudes of the terdiurnal in figure 5.

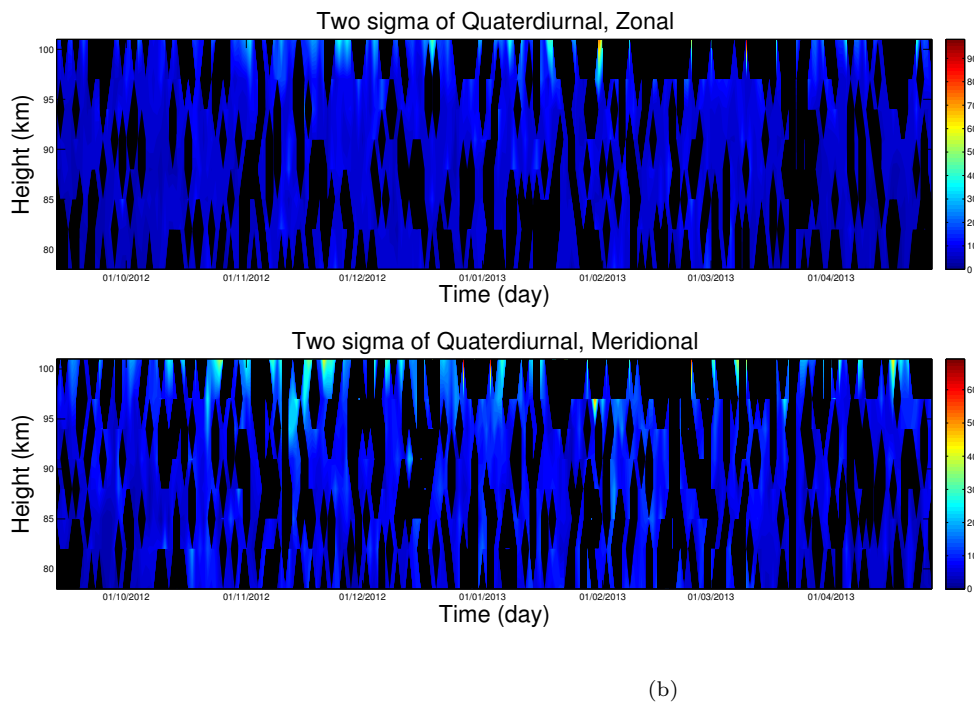
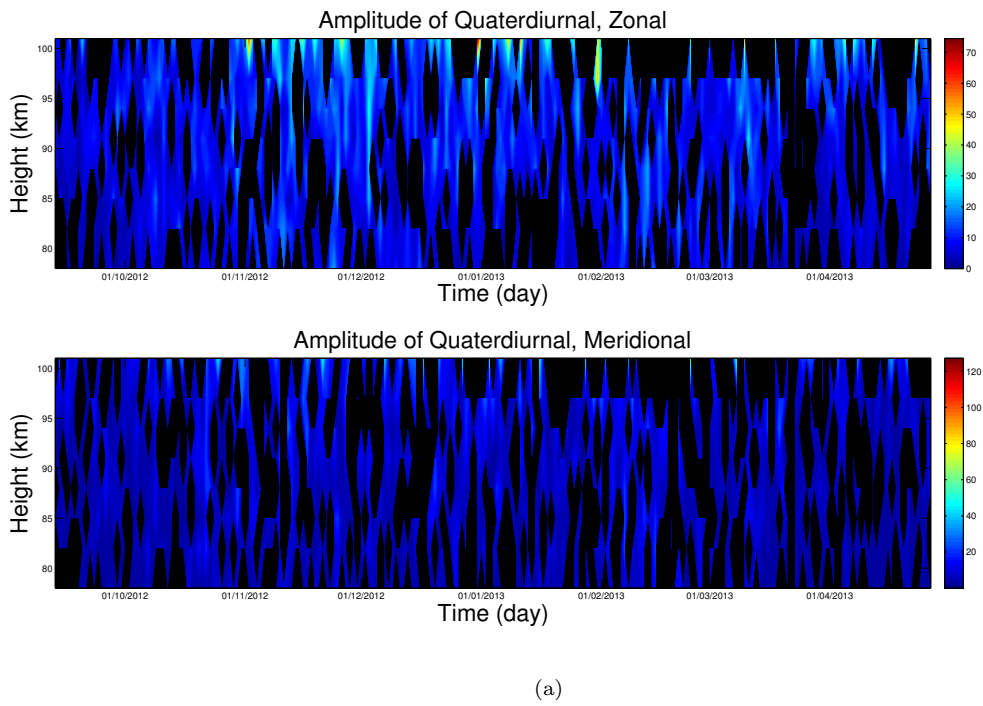


Figure 5.7: (a) Significant amplitudes found for the 6-hour tidal wave in the period from September 10th 2012 until April 30th 2013. (b)  $2\sigma$  error of the amplitudes.

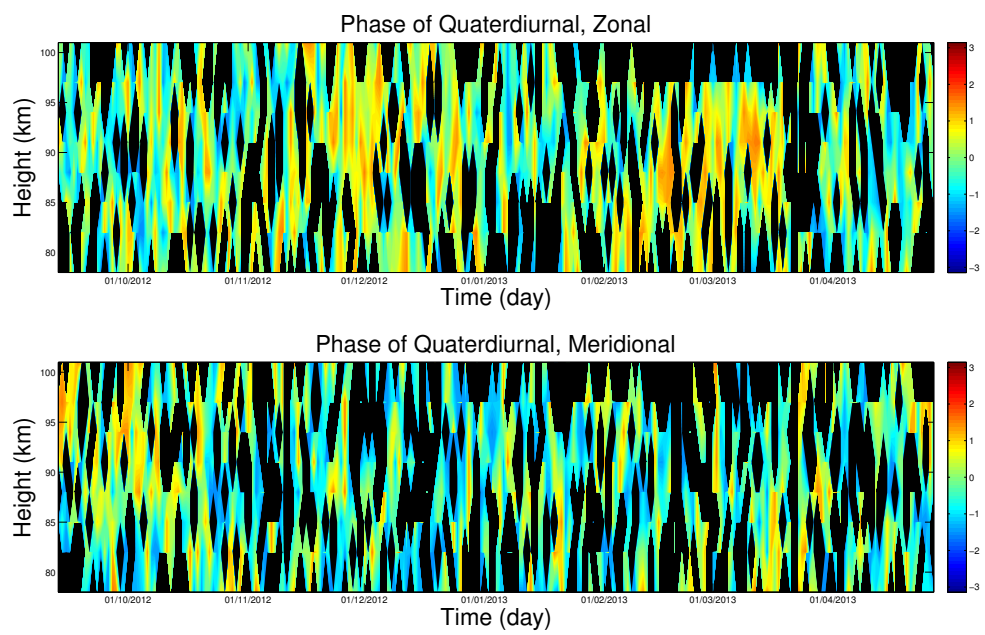


Figure 5.8: phase for the amplitudes found in figure 5.7

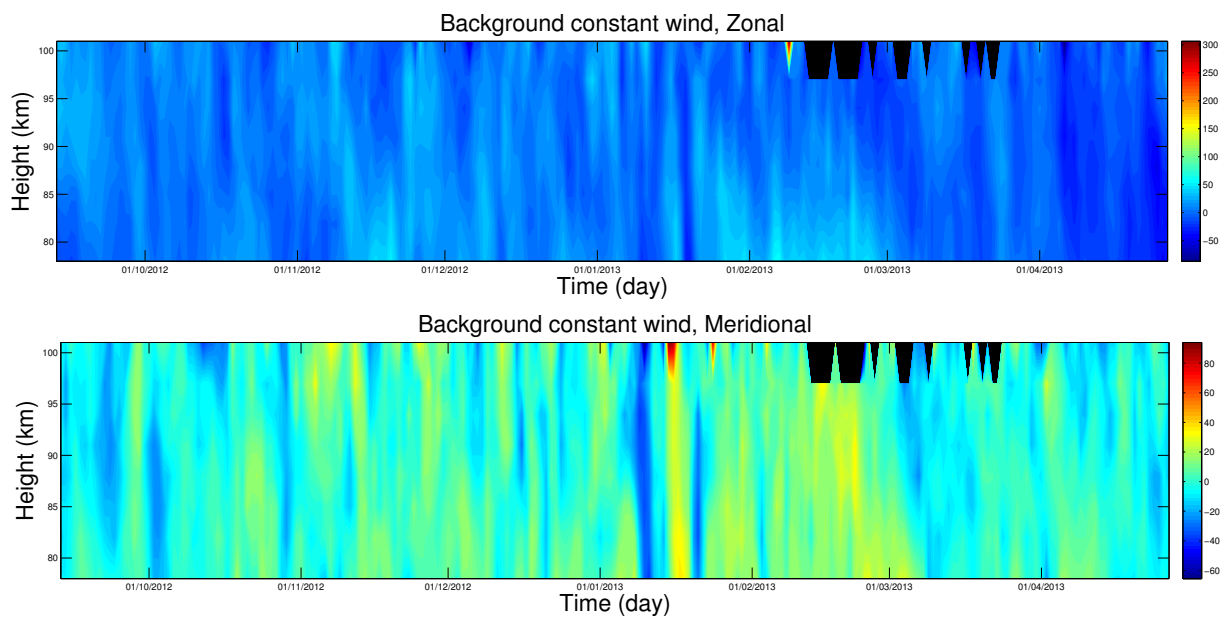
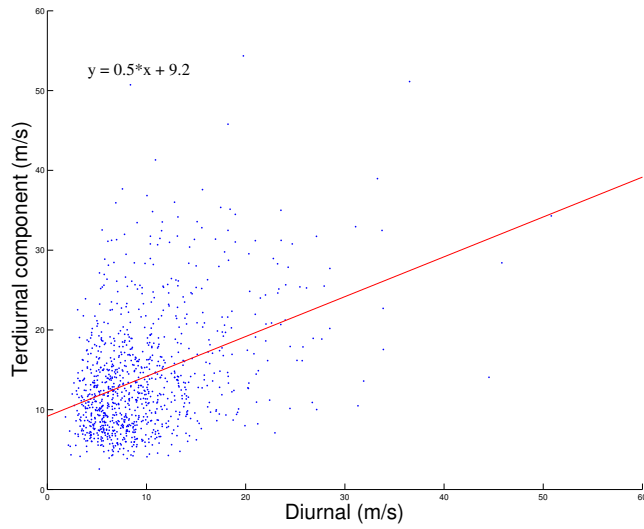
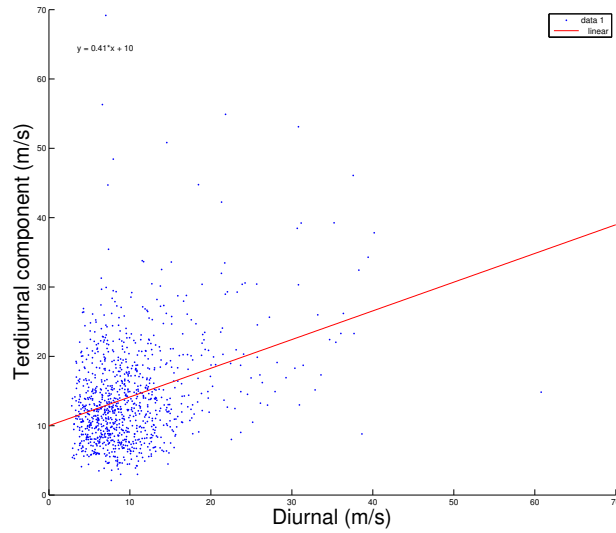


Figure 5.9: The background wind at different points in the atmosphere, fitted in the code as a constant.

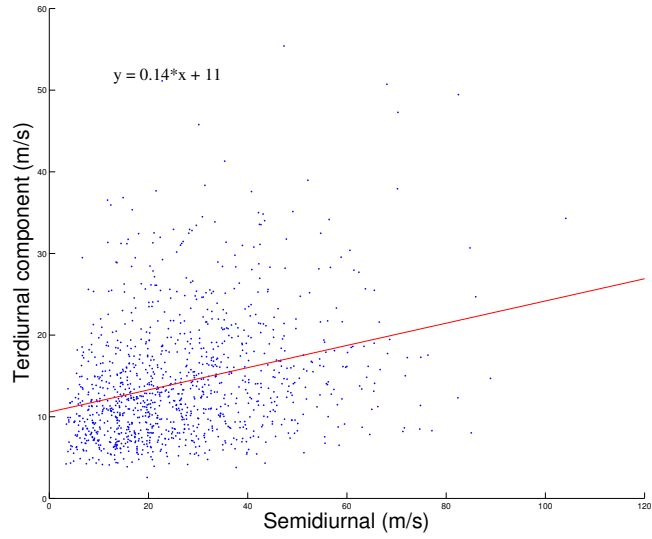


(a)

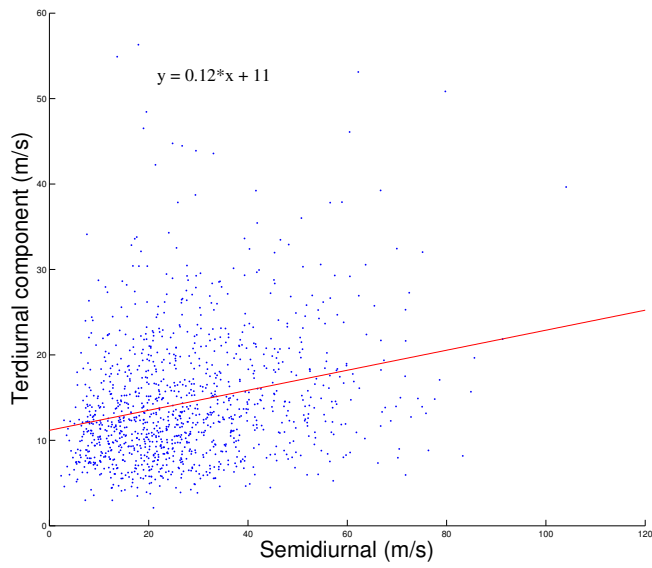


(b)

Figure 5.10: Scatter plot with the amplitudes of the terdiurnal plottet against the amplitude of the diurnal tide. (a) Zonal, (b) Meridional.

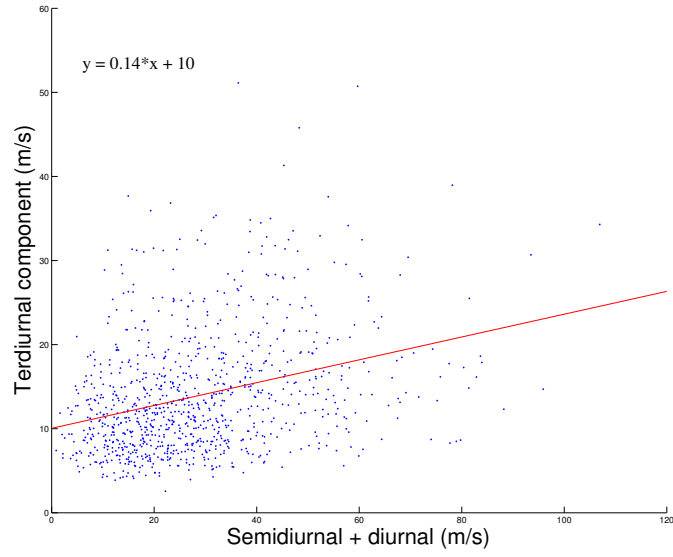


(a)

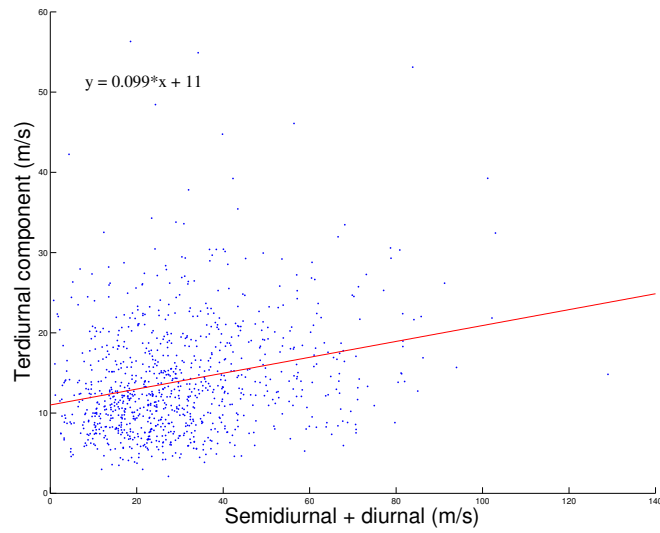


(b)

Figure 5.11: Scatter plot with the amplitude of the terdiurnal plotted against the amplitude of the semidiurnal. (a) zonal, (b) meridional



(a)



(b)

Figure 5.12: scatter plot of the terdiurnal amplitude against the semidiurnal+diurnal. (a) Zonal, (b) meridional



## Chapter 6

# Discussion

Since this project was meant to focus on the high frequency components of the atmospheric tidal oscillations, this will also be the main focus of this discussion. However some interesting features appears also in the other parts of the result. By looking at the phase plot of the semidiurnal in figure 5.4 one can see that something is happening in early January. Just before that period the background wind has a clear change in the meridional part, as can be seen in figure 5.9. This is apparently a result of a stratwarming. As previously stated this is not the main focus of this project, so this will just be pointed out and not investigated any further here.

It is also worth mentioning that the largest values of the diurnal was found at times where the semidiurnal was also approaching its maximum values at 99-104 on 16.Jan. 2013 for the meridional and on 6. April 2013 for the zonal. For the 6. April values, both also show high  $2\sigma$  values ( $\approx 70m/s$ , while for the 16. January value the value for  $2\sigma$  is in the order of  $\approx 40m/s$ ).

Some discussion about the removed datapoints should be done. The extremely high amplitudes are highly unlikely to be real, however the Matlab-routine didn't remove them properly as the error was small enough for them to be real. It might be a result of some bad datapoints at small zenith angles. If the assumption of no vertical wind breaks is invalid at some time due to some atmospheric situation, this would result in a line of sight velocity that is higher than normal. If three meteors enters this region at that time, the error in the U and V component would still be low and the weighting should stay fairly high throughout the fitting routine. If there are some well placed NaN's in the dataset around where the oscillation should be at it's maximum, and some of the datapoints in between the zero and the maximum have higher values because of vertical motion, this may cause a large fit to have a small error. Take for example the six hour, where 12 values need to be present for a fit over 18 hours. If 6 of these are zeros and a few of the other points have a high value, while none of them are where the maximum would be, a large fit can get a small

error. Over 233 days and 8 heights it is not unlikely that this could occur.

A good amount of amplitudes was found for the terdiurnal, at least for the altitudes below 99 km. Figures 5.10, 5.11 and 5.12 shows how the amplitude of the terdiurnal changes with changing amplitude for the diurnal, the semidiurnal and the two combined. All these plots show a tendency for the terdiurnal tide to be larger when the two others are large, which suggests that there is a common driving force of these waves. However this isn't a clear cut connection, as can be seen by the large spread in the scatter plots. Based on this there might be other variables then the thermal heating deciding the amplitude of the terdiurnal, one possibility being gravity waves propagating upwards in the atmosphere.

Some days one can see a clear impact of the terdiurnal wave, and an example of this is the 9th of October 2012. The plot of U and V for this day clearly shows that more then a semidiurnal wave is present at this date. By plotting the fits together with the data (figure 6.1 one can investigate what is happening here. By looking at figure 5 this date doesn't stand out at all, however by looking at figure ?? the red data show that the amplitude of the terdiurnal at this point is much larger compared to the semidiurnal amplitude then what it normally is, however the terdiurnal itself is less then two times its average value. This goes to show that the terdiurnal in this point is so visible in this data not only because the terdiurnal is larger then it normally is, but the semidiurnal is also much smaller then what is normal. By looking at figure 6.1 we can see that the amplitude is less then  $20\frac{m}{s}$ . This data point, and others like it, show that the amplitude of the terdiurnal can at times be larger then that of semidiurnal.

In order to further accept the results as valid there was done a Fourier analysis of the residuals after the semidiurnal was removed from the datasets. Looking at one for the zonal part at 93-96 km in figure ?? one can see that the main residing components are around  $f = 0.125$ , which is where the terdiurnal should be. The quaterdiurnal should be around 0.17, and at times one can see that there is a peak here as well, although this isn't as visible as it is for the terdiurnal. The Fourier routine isn't ideal, as a Lomb-Scargle would be better, however the version of Matlab that was used in this project did not have an in-built Lomb-Scargle function, and there was not enough time to create one. The Fourier routine that was used sets all NaN-values to zero, which may introduce frequencies that would not otherwise be there. With this in mind the figure included in this project is from a range where there was found semidiurnal amplitudes for 94.8% of the dates, which suggests that there was fewer NaN-values there then in for example the 99-104-range, where the semidiurnal could only be fitted to 76.8% of the days.

As for the yearly variation in the amplitudes for the terdiurnal and quaterdiurnal components, the amount of months of data that was available for this project could be better. For the eight months that were analyzed it appears that the lowest values for most of the ranges for both components were found in

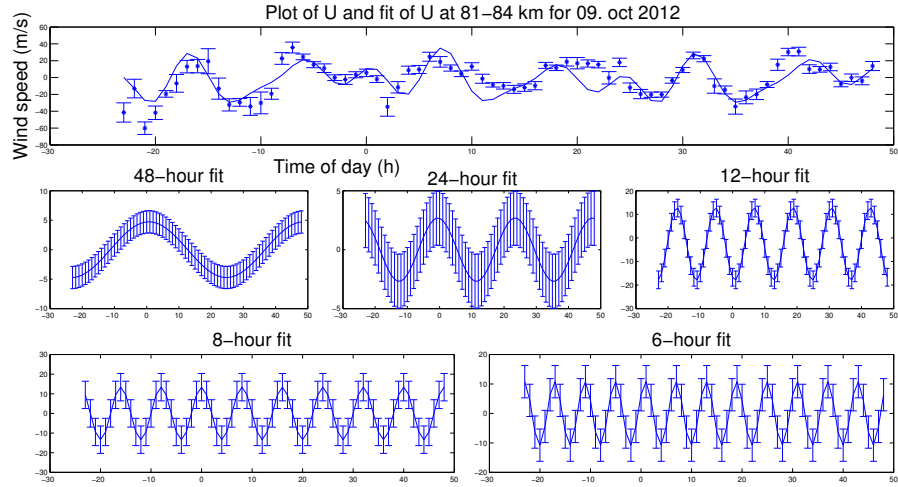


Figure 6.1: Plot of the data and the fits for 81-84 km, 09.Oct 2012

September. This does not really say much, as I haven't looked at several years of data. The largest monthly averages were found in February for the terdiurnal at almost all altitudes both for the zonal and the meridional component. For the quaterdiurnal component this tendency was not as strong, however February was the only month where all altitudes except one had average amplitude above  $10m/s$ . It should be mentioned that the average values in table 5.1-?? are calculated only for the significant values found, not with zero for the days where they were not found to be significant.

In general it should be pointed out that the results from the 99-104 km range shows a tendency to be uncertain. The fitting routine could not find nearly as many results in this region as it could in the other regions, and the highest values for all the components were found in this region (when including the points that were excluded from the plot.). This is due to the low number of meteors that burn up in this region, which leads to high uncertainty for the U and V-fits in this region. One thing that was not done in this project, is a double-fit of the U and V data. By first fitting the U and V, look at what values that would give for the  $V_{rad}$ , exclude the points that are outside some set tolerance level and then fit the U and V again, one would most likely loose even more data points for U and V, however it would increase the accuracy of these values.

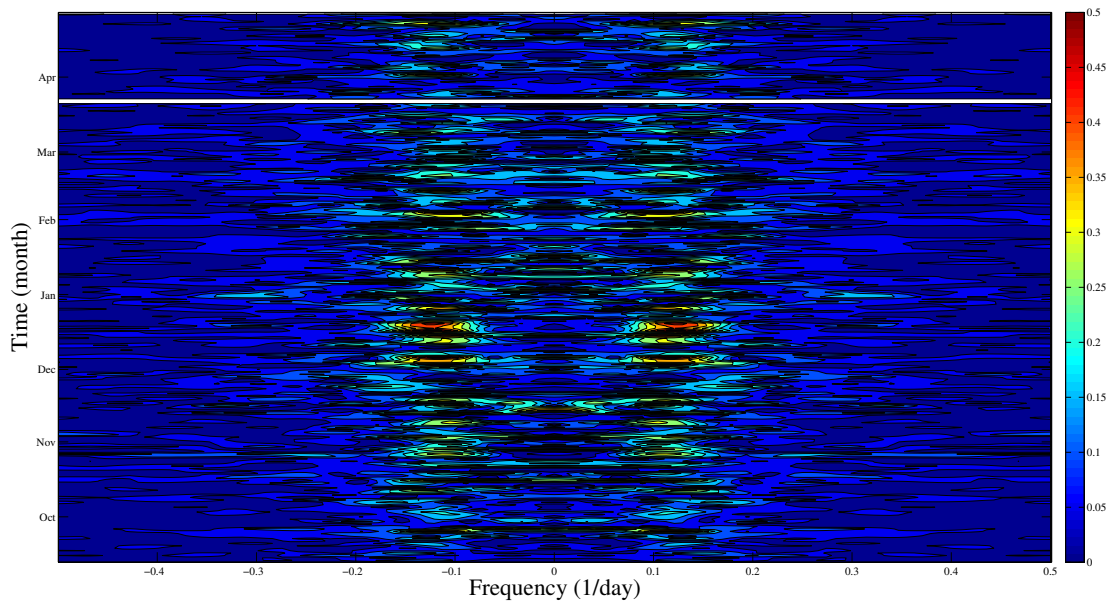


Figure 6.2: Caption for FourierU-93-96

## Chapter 7

# Conclusion

Through the least-squares fitting routines there was found occurrences of the terdiurnal and quaterdiurnal tidal components in the winds in the MLT-region. For all the components the amplitudes generally increases with altitude, as well as the  $2\sigma$  values. The average values found for the terdiurnal ranged from (increasing with altitude)  $9.1 - 25.9m/s$  and  $10.1 - 26.0m/s$  for the zonal and meridional part of the altitudes that were investigated. For the quaterdirunal the average values also increased with altitude and were found to be  $7.6 - 22.8m/s$  and  $7.7 - 28.0m/s$  for the zonal and meridional component.

The amplitude of the terdiurnal tide was at times found to be of the same magnitude and even larger then the semidiurnal tide. This suggests that there may be other driving forces of the terdiurnal then the thermal forcing from the sun, as one would also expect the semidiurnal to react similarly. One possibility may be that it is related to gravity waves propagating in the atmosphere. To further investigate this, one should see how the magnitude of the terdiurnal varies in relation to gravity wave activity in the atmosphere.



# Bibliography

- [1] Lindzen, R.S. *Atmospheric Tides*, Annual reviews, 1979
- [2] Smith, A.K. *Structure of the Terdiurnal Tide at 95 km*, Geophysical research letters, 2000.
- [3] Smith, A.K., Ortland, D. A. *Modeling and Analysis of the Structure and Generation of the Terdiurnal Tide*, 2001.
- [4] Forbes, J.M. *Vertical coupling of the Semidiurnal tide in the Earth's atmosphere*, 2009
- [5] Lieberman, R.S. *An overview of middle atmosphere tides*, HEPPA (International high energy particle precipitation in the atmosphere workshop), 2009
- [6] Beldon, C.L., Muller, H.G., Mitchell, N.J. *The 8-hour tide in the mesosphere and lower thermosphere over the UK, 1988-2004*, Journal of Atmospheric and Solar-Terrestrial Physics, 2006
- [7] Thayaparan, T. *The terdiurnal tide in the mesosphere and lower thermosphere over London, Canada*, Journal of geophysical research, 1997
- [8] Hibbins, R. E., Espy, P.J., Jarvis, M.J., Riggan, D.M., Fritts, D.C. *A climatology of tides and gravity wave variance in the MLT above Rothera, Antarctica obtained by MF radar*, Journal of Atmospheric and Solar-Terrestrial Physics, 2007
- [9] Kolnes, N.H. *Doppler Imaging Of Gravity Waves*, Specialization project NTNU, 2012.
- [10] Hocking, W.K., et al. *Real time determination of meteor-related parameters utilizing modern technology*", Journal of Atmospheric and Solar-Terrestrial Physics, 63 (2001)
- [11] Atmospheric group's homepage, <http://home.phys.ntnu.no/bbrukdef/prosjekter/atmosfys/webpages/SKiYMET-wind.php>



# Appendix A

## Matlab code

### A.1 Main program file and control file when finding the amplitudes and phases

```
function [ amps, F]=getAmps(U,Uw,I ,oldAmps, fileName )
%amps(U,Uw,I,oldAmps,filename) takes the values in U, fits a 48,24,12,8&6
%hour wave to it as well as a constant using weighting Uw, over I times the
%wavelength of the components. It uses oldAmps as starting values for the
%fit and also stores the original U wit weighting to filename. Outputs are
%the amplitudes and phases of the components with 2sigma confidence bounds
%in amps and/or the fourier of the

amps=zeros(11,3);           %Amplituddes, phi-values and value of the constant
%[A48 A24 A12 A8 A6 Phi48 Phi24 Phi12 Phi8 Phi6 C],
%with confidence intervals in amps(:,2:3)

f48=@(x,amp,phi) amp*cos(x*2*pi/48+phi);
f24=@(x,amp,phi) amp*cos(x*2*pi/24+phi);
f12=@(x,amp,phi,C) C+amp*cos(x*2*pi/12+phi);
f8=@(x,amp,phi) amp*cos(x*2*pi/8+phi);
t=(1:(2*I+1)*24)';
Utemp(:,1)=U(:);
Utemp(:,2)=Uw(:);

    dlmwrite(fileName, Utemp(:,:), 'delimiter', '\t', 'precision', 6);
% %Saving U to textfile, with weighting Uw.

[tempAmp,tempClevel] = fit48(t(12:((2*I+1)*24-12)),U(12:((2*I+1)*24-12))...
,Uw(12:((2*I+1)*24-12)),[oldAmps(1),oldAmps(2),oldAmps(3),oldAmps(11),...
oldAmps(6),oldAmps(7),oldAmps(8)]);%Fit-function.
```

```

%They all pretty much look the same, but with different wavelengths.
amps(1,1)=tempAmp(1); amps(1,2)=tempClevel(1,1); amps(1,3)=tempClevel...
(2,1);%Saves the values found for the amplitudes to the matrix amps.
amps(6,1)=tempAmp(5); amps(6,2)=tempClevel(1,5); amps(6,3)=tempClevel(2,5);

```

```

if ~isnan(tempClevel(1))&&tempAmp(1)>0.5*(tempClevel(2,1)-tempClevel(1,1));
Utemp(:,1)=Utemp(:,1)-f48(t(:),tempAmp(1),tempAmp(4)); %Removes the 48-hour
end %from the dataset, if it is significant.

```

```

[tempAmp, tempClevel]=fit24(t((2*I+1)*12-I*12:(2*I+1)*12+I*12),...
Utemp((2*I+1)*12-I*12:(2*I+1)*12+I*12,1),Utemp((2*I+1)*12-I*12:(2*I+1)*...
12+I*12,2),[tempAmp(2),tempAmp(3),tempAmp(4),tempAmp(6),tempAmp(7)]);
amps(2,1)=tempAmp(1); amps(2,2)=tempClevel(1,1); amps(2,3)=tempClevel(2,1);
amps(7,1)=tempAmp(4); amps(7,2)=tempClevel(1,4); amps(7,3)=tempClevel(2,4);

```

```

if ~isnan(tempClevel(1))&&tempAmp(1)>0.5*(tempClevel(2,1)-tempClevel(1,1));
Utemp(:,1)=Utemp(:,1)-f24(t(:),tempAmp(1),tempAmp(4));%Removes the
end %diurnal wave

```

```

[tempAmp, tempClevel]=fit12(t((2*I+1)*12-I*6:(2*I+1)*12+I*6),...
Utemp((2*I+1)*12-I*6:(2*I+1)*12+I*6,1),Utemp((2*I+1)*12-...
I*6:(2*I+1)*12+I*6,2),[tempAmp(2),tempAmp(3),tempAmp(5)]);
amps(3,1)=tempAmp(1); amps(3,2)=tempClevel(1,1); amps(3,3)=tempClevel(2,1);
amps(8,1)=tempAmp(3); amps(8,2)=tempClevel(1,3); amps(8,3)=tempClevel(2,3);
amps(11,1)=tempAmp(2); amps(11,2)=tempClevel(1,2); amps(11,3)=tempClevel(2,2);

```

```

if ~isnan(tempClevel(1))&&tempAmp(1)>0.5*(tempClevel(2,1)-tempClevel(1,1));
Utemp(:,1)=Utemp(:,1)-f12(t(:),tempAmp(1),tempAmp(3),tempAmp(2));
end %Removes the semidiurnal, if significant.

```

```

F=fourierAnalyse(Utemp((2*I+1)*12-I*4:(2*I+1)*12+I*4,1),t((2*I+1)*12-...
I*4:(2*I+1)*12+I*4,1)); %Fourier analysis of U.

```

```

[tempAmp, tempClevel]=fit8(t((2*I+1)*12-I*4:(2*I+1)*12+I*4,1),...
Utemp((2*I+1)*12-I*4:(2*I+1)*12+I*4,1),Utemp((2*I+1)*12-...
I*4:(2*I+1)*12+I*4,2),[oldAmps(4),oldAmps(9)]);
amps(4,1)=tempAmp(1); amps(4,2)=tempClevel(1,1); amps(4,3)=tempClevel(2,1);
amps(9,1)=tempAmp(2); amps(9,2)=tempClevel(1,2); amps(9,3)=tempClevel(2,2);

```

```

if ~isnan(tempClevel(1))&&tempAmp(1)>0.5*(tempClevel(2,1)-tempClevel(1,1));
Utemp(:,1)=Utemp(:,1)-f8(t(:),tempAmp(1),tempAmp(2));
end%Removes the terdiurnal, if significant.

```

```

[tempAmp, tempClevel]=fit6(t((2*I+1)*12-I*3:(2*I+1)*12+I*3),...
Utemp((2*I+1)*12-I*3:(2*I+1)*12+I*3,1),Utemp((2*I+1)*12-...
I*3:(2*I+1)*12+I*3,2),[oldAmps(5),oldAmps(10)]);

```

```
amps(5,1)=tempAmp(1); amps(5,2)=tempClevel(1,1); amps(5,3)=tempClevel(2,1);
amps(10,1)=tempAmp(2); amps(10,2)=tempClevel(1,2); amps(10,3)=tempClevel(2,2);
```

```
close all
```

```
clear all
```

```
%This file runs through datasets from the SKiYMET radar and extracts the
%amplitudes for diurnal, semidiurnal, terdiurnal, 48-hour and 6-hour tide.
%These values are stored in matrices.
```

```
I=3; %Number of wavelengths to evaluate for the different frequencies
```

```
formatOut='yyyymmdd';
```

```
start_date = datenum('09/10/2012'); %Deciding start and end date.
```

```
end_date = datenum('04/30/2013');
```

```
dates = (start_date:1:end_date);
```

```
N=length(dates); % Number of days to evaluate
```

```
ampU=zeros(11,3,8);
```

```
ampV=zeros(11,3,8);
```

```
fourierU=zeros(125,N,8);
```

```
fourierV=zeros(125,N,8);
```

```
UAmp6=zeros(N,8,3);
```

```
%Creating matrices where values for amplitude and
```

```
UAmp8=zeros(N,8,3);
```

```
%phase for different frequencies can be stored
```

```
UAmp12=zeros(N,8,3);
```

```
%for later evaluation. Both for U and V.
```

```
UAmp24=zeros(N,8,3);
```

```
UAmp48=zeros(N,8,3);
```

```
Uconst=zeros(N,8,3);
```

```
UPhi6=zeros(N,8,3);
```

```
UPhi8=zeros(N,8,3);
```

```
UPhi12=zeros(N,8,3);
```

```
UPhi24=zeros(N,8,3);
```

```
UPhi48=zeros(N,8,3);
```

```
VAmp6=zeros(N,8,3);
```

```
VAmp8=zeros(N,8,3);
```

```
VAmp12=zeros(N,8,3);
```

```
VAmp24=zeros(N,8,3);
```

```
VAmp48=zeros(N,8,3);
```

```
Vconst=zeros(N,8,3);
```

```
VPhi6=zeros(N,8,3);
```

```
VPhi8=zeros(N,8,3);
```

```
VPhi12=zeros(N,8,3);
```

```
VPhi24=zeros(N,8,3);
```

```
VPhi48=zeros(N,8,3);
```

```
U=zeros((2*I+1)*24,8,3);
```

```

V=zeros((2*I+1)*24,8,3);

for Ncurr=1:N

    date = datestr( dates(Ncurr),formatOut );
    NAME=strcat( 'mpdfiles/mp',date, '.trondheim.mpd' );
    FID=fopen( NAME );
    FORMAT= '%s%s%s%f%f%f%f%f%f%f%f%f%f%f%f%f';
    DATA = textscan( FID,FORMAT, 'HeaderLines',29);
    DATA{1,1}=strrep( DATA{1,1}, '/' , '' ); %These lines find the files with
    DATA{1,1}=str2double( DATA{1,1} ); %data from the meteor-radar, and
    DATA{1,2}=strrep( DATA{1,2}, ':' , '' ); %read the relevant parts of them
    DATA{1,2}=str2double( DATA{1,2} ); %into the matlab-variable DATA.
    DATA=cell2mat( DATA ); %From this the U's and V's are found
    fclose( FID ); %and added into a variable with 7
    U(1:24*2*I, :, 1:3)=U(25:(2*I+1)*24, :, 1:3); %days worth of data. This way
    V(1:24*2*I, :, 1:3)=V(25:(2*I+1)*24, :, 1:3); %the day in question will be
    [newU, newV]=fillUV( DATA ); %in the middle of the matrix.
    U((2*I)*24+1:(2*I+1)*24, :, :)=newU( :, :, : );
    V(24*(2*I)+1:(2*I+1)*24, :, :)=newV( :, :, : );
    clear DATA;
    clear FID;
    clear FORMAT;
    clear newU;
    clear newV;

% if Ncurr>= 4&&&Ncurr<N-2;
% datestr( dates(Ncurr), 'dd/mm/yyyy' ) %This was used if the U's and V's
% [U,V]=loadUV( date ); %were already saved to textfiles.
% %but I wanted to try something
% %new elsewhere in the code.

for i=1:8
    fileName=strcat( datestr( dates(Ncurr),formatOut), 'U2',int2str(i) );
    [ampU(1:11,1:3,i),fourierU(:,Ncurr,i)]= getAmps(U(:,i,1),U(:,i,2),I, ...
    ampU(:,1,i), fileName );

    UAmp6(Ncurr,i,1)=ampU(5,1,i); %This is not the most elegant way to store
    UAmp6(Ncurr,i,2)=ampU(5,2,i); %these values in their respective matrices,
    UAmp6(Ncurr,i,3)=ampU(5,3,i); %but it sure does the trick.

    UAmp8(Ncurr,i,1)=ampU(4,1,i);
    UAmp8(Ncurr,i,2)=ampU(4,2,i);
    UAmp8(Ncurr,i,3)=ampU(4,3,i);

    UAmp12(Ncurr,i,1)=ampU(3,1,i);

```

```

UAmp12(Ncurr , i , 2)=ampU(3 , 2 , i );
UAmp12(Ncurr , i , 3)=ampU(3 , 3 , i );

UAmp24(Ncurr , i , 1)=ampU(2 , 1 , i );
UAmp24(Ncurr , i , 2)=ampU(2 , 2 , i );
UAmp24(Ncurr , i , 3)=ampU(2 , 3 , i );

UAmp48(Ncurr , i , 1)=ampU(1 , 1 , i );
UAmp48(Ncurr , i , 2)=ampU(1 , 2 , i );
UAmp48(Ncurr , i , 3)=ampU(1 , 3 , i );

UPhi6(Ncurr , i , 1)=ampU(10 , 1 , i );
UPhi6(Ncurr , i , 2)=ampU(10 , 2 , i );
UPhi6(Ncurr , i , 3)=ampU(10 , 3 , i );

UPhi8(Ncurr , i , 1)=ampU(9 , 1 , i );
UPhi8(Ncurr , i , 2)=ampU(9 , 2 , i );
UPhi8(Ncurr , i , 3)=ampU(9 , 3 , i );

UPhi12(Ncurr , i , 1)=ampU(8 , 1 , i );
UPhi12(Ncurr , i , 2)=ampU(8 , 2 , i );
UPhi12(Ncurr , i , 3)=ampU(8 , 3 , i );

UPhi24(Ncurr , i , 1)=ampU(7 , 1 , i );
UPhi24(Ncurr , i , 2)=ampU(7 , 2 , i );
UPhi24(Ncurr , i , 3)=ampU(7 , 3 , i );

UPhi48(Ncurr , i , 1)=ampU(6 , 1 , i );
UPhi48(Ncurr , i , 2)=ampU(6 , 2 , i );
UPhi48(Ncurr , i , 3)=ampU(6 , 3 , i );

Uconst(Ncurr , i , 1)=ampU(11 , 1 , i );
Uconst(Ncurr , i , 2)=ampU(11 , 2 , i );
Uconst(Ncurr , i , 3)=ampU(11 , 3 , i );

fileName=strcat( datestr( dates(Ncurr) , formatOut) , 'V2' , int2str(i) );
[ampV(1:11 , 1:3 , i) , fourierV(: , Ncurr , i)]=getAmps(V(: , i , 1) , V(: , i , 2) , I , ...
ampV(: , 1 , i) , fileName );

VAmp6(Ncurr , i , 1)=ampV(5 , 1 , i );
VAmp6(Ncurr , i , 2)=ampV(5 , 2 , i );
VAmp6(Ncurr , i , 3)=ampV(5 , 3 , i );

VAmp8(Ncurr , i , 1)=ampV(4 , 1 , i );
VAmp8(Ncurr , i , 2)=ampV(4 , 2 , i );
VAmp8(Ncurr , i , 3)=ampV(4 , 3 , i );

```

```

VAmp12(Ncurr , i ,1)=ampV(3 ,1 , i );
VAmp12(Ncurr , i ,2)=ampV(3 ,2 , i );
VAmp12(Ncurr , i ,3)=ampV(3 ,3 , i );

VAmp24(Ncurr , i ,1)=ampV(2 ,1 , i );
VAmp24(Ncurr , i ,2)=ampV(2 ,2 , i );
VAmp24(Ncurr , i ,3)=ampV(2 ,3 , i );

VAmp48(Ncurr , i ,1)=ampV(1 ,1 , i );
VAmp48(Ncurr , i ,2)=ampV(1 ,2 , i );
VAmp48(Ncurr , i ,3)=ampV(1 ,3 , i );

VPhi6(Ncurr , i ,1)=ampV(10 ,1 , i );
VPhi6(Ncurr , i ,2)=ampV(10 ,2 , i );
VPhi6(Ncurr , i ,3)=ampV(10 ,3 , i );

VPhi8(Ncurr , i ,1)=ampV(9 ,1 , i );
VPhi8(Ncurr , i ,2)=ampV(9 ,2 , i );
VPhi8(Ncurr , i ,3)=ampV(9 ,3 , i );

VPhi12(Ncurr , i ,1)=ampV(8 ,1 , i );
VPhi12(Ncurr , i ,2)=ampV(8 ,2 , i );
VPhi12(Ncurr , i ,3)=ampV(8 ,3 , i );

VPhi24(Ncurr , i ,1)=ampV(7 ,1 , i );
VPhi24(Ncurr , i ,2)=ampV(7 ,2 , i );
VPhi24(Ncurr , i ,3)=ampV(7 ,3 , i );

VPhi48(Ncurr , i ,1)=ampV(6 ,1 , i );
VPhi48(Ncurr , i ,2)=ampV(6 ,2 , i );
VPhi48(Ncurr , i ,3)=ampV(6 ,3 , i );

Vconst(Ncurr , i ,1)=ampV(11 ,1 , i );
Vconst(Ncurr , i ,2)=ampV(11 ,2 , i );
Vconst(Ncurr , i ,3)=ampV(11 ,3 , i );
% end %This "end" needs to be here if the program runs with already found
end %values for U and V.
end

```

## A.2 Codes to sort the data and fit U's and V's

```
function [U,V]=loadUV(date)  
% loadUV(date) Loads the file with U and V stripped of the 48,24 & 12 hour  
% wave. date in the form yyyyymmdd.  
% This was used to load in data that was already stored for U and V, in  
% order to make the project file run faster. It also comes in handy if one  
% wishes to examine a particular date at a later time.
```

```
for i=1:8  
  
    NAMEU=strcat(date, 'U2',int2str(i));  
    FID=fopen(NAMEU);  
    FORMAT='%f%f';  
    DATAU = textscan(FID,FORMAT);  
    DATAU=cell2mat(DATAU);  
    fclose(FID);  
    U(:,i,:)=DATAU(:,,:);  
  
    NAMEV=strcat(date, 'V2',int2str(i));  
    FIDV=fopen(NAMEV);  
    FORMAT='%f%f';  
    DATAV = textscan(FIDV,FORMAT);  
    DATAV=cell2mat(DATAV);  
    fclose(FIDV);  
    V(:,i,:)=DATAV(:,,:);  
  
end
```

```
function [U,V] = fillUV(DATA)  
%This function extracts U and V components from different heights and  
%timeperioodes of the dataset DATA. These are stored the 24x8x3 matrices U  
%and V, containing the value, lower confidence bound and upper confidence  
%bound for 24 hours and 8 different height intervals.  
U=zeros(24,8,3);  
V=zeros(24,8,3);  
TH=getTH1(DATA); %Collects the time and height indicies for DATA.  
    %Originally called getTH, but got modified and renamed.  
    %The same thing happened to getSpeed->getSpeed2.
```

```
for i=1:24  
    for j=1:8  
        l=lengde(TH(i,j,:));  
        if l>=3;  
            x=DATA(TH(i,j,1:1),7);
```

```

        y=DATA(TH(i,j,1:1),8);
        v=DATA(TH(i,j,1:1),5);
        W=0*x+1;%Optional weighting of the different points. No weighting
        R=getSpeed2(x,y,v,W);%was used here in the project, but is easily
        coeff=coeffvalues(R);%implemented if one wishes to do it.
        cint=confint(R,0.68);%2sigma chosen as confidence level.
        else
            cint=[NaN, NaN;NaN,NaN];
            coeff=[NaN NaN];
        end
        U(i,j,1)=coeff(1,1);
        V(i,j,1)=coeff(1,2);
        U(i,j,2)=1/(coeff(1,1)-cint(1,1))^2;
        V(i,j,2)=1/(cint(2,2)-coeff(1,2))^2;
    end
end

function TH = getTH1(DATA)
%This function takes the dataset DATA and returns indicies in TH sorted in
%height and time.
T1=findTimeIndex(DATA); %Finds the first timeindicies for each hour of data.
K1=1;
Ks=[1 1 1 1 1 1 1 1];%These are indicies for the different heights.
for i = 1:24;
    K2=T1(i); %Starting index for each hour.
    for j =K1:K2 ;
        H=DATA(j,4);
        if DATA(j,6)<=5.5
            if H>=81 && H<99 && DATA(j,9)==1&&DATA(j,7)>15&&DATA(j,7)<55;%These
                J=floor(1/3*(H-81))+2;%are the middle height indicies.
                TH(i,J,Ks(J))=j;
                Ks(J)=Ks(J)+1;
            elseif H>=76&&H<81 && DATA(j,9)==1&&DATA(j,7)>15&&DATA(j,7)<55;
                TH(i,1,Ks(1))=j;%These heights weren't regular, in that they
                Ks(1)=Ks(1)+1;contained% 5km's instead of 3, and they therefore
                % had to be found in a different manner.
            elseif H>=99&&H<104 && DATA(j,9)==1&&DATA(j,7)>15&&DATA(j,7)<55;

                TH(i,8,Ks(8))=j;
                Ks(8)=Ks(8)+1;
            end
        end
    end
    K1=K2+1;
    Ks=[1 1 1 1 1 1 1 1];
end
end

```

```

function timeIndicies = findTimeIndex(DATA)
%This function isn't pretty, but it's relatively fast and finds the
%starting index for different hours of the day. This was made very early on
%in the project and still worked, so I felt no need to revisit it.
l=size(DATA,1);
timeIndicies=zeros(1,24)';
timeIndicies(24)=1;
i=1;
reachedEnd=false;
while i<l && reachedEnd == false;
    D1=DATA(i,2);
    D2=DATA(i+1,2);
    if D1 <= 10000 && D2>10000;
        timeIndicies(1)=i;
    elseif D1 <= 20000 && D2>20000;
        timeIndicies(2)=i;
    elseif D1 <= 30000 && D2>30000;
        timeIndicies(3)=i;
    elseif D1 <= 40000 && D2>40000;
        timeIndicies(4)=i;
    elseif D1 <= 50000 && D2>50000;
        timeIndicies(5)=i;
    elseif D1 <= 60000 && D2>60000;
        timeIndicies(6)=i;
    elseif D1 <= 70000 && D2>70000;
        timeIndicies(7)=i;
    elseif D1 <= 80000 && D2>80000;
        timeIndicies(8)=i;
    elseif D1 <= 90000 && D2>90000;
        timeIndicies(9)=i;
    elseif D1 <= 100000 && D2>100000;
        timeIndicies(10)=i;
    elseif D1 <= 110000 && D2>110000;
        timeIndicies(11)=i;
    elseif D1 <= 120000 && D2>120000;
        timeIndicies(12)=i;
    elseif D1 <= 130000 && D2>130000;
        timeIndicies(13)=i;
    elseif D1 <= 140000 && D2>140000;
        timeIndicies(14)=i;
    elseif D1 <= 150000 && D2>150000;
        timeIndicies(15)=i;
    elseif D1 <= 160000 && D2>160000;
        timeIndicies(16)=i;
    elseif D1 <= 170000 && D2>170000;
        timeIndicies(17)=i;

```

```

elseif D1 <= 180000 && D2>180000;
    timeIndicies(18)=i;
elseif D1 <= 190000 && D2>190000;
    timeIndicies(19)=i;
elseif D1 <= 200000 && D2>200000;
    timeIndicies(20)=i;
elseif D1 <= 210000 && D2>210000;
    timeIndicies(21)=i;
elseif D1 <= 220000 && D2>220000;
    timeIndicies(22)=i;
elseif D1 <= 230000 && D2>230000;
    timeIndicies(23)=i;
    reachedEnd=true;
end
i=i+1;
end

```

```

function [fitResults , gof] = getSpeed2(x,y,Vr,W)
%This function fits a U and V to the datapoints in Vr based on the zenith
%and azimuth angles x and y. It is possible to use the weighting W, however
%this wasn't done in this project.
ft=fittype('U*sind(x)*cosd(y)+V*sind(x)*sind(y)', 'indep',{ 'x','y' },...
'depend','z');
opts = fitoptions(ft);
opts.Display='off';
opts.Lower=[-Inf -Inf];
opts.Startpoint=[0.7 0.6];
opts.Upper=[Inf Inf];
% opts.Weight=W; %If one wishes to weight the points, one can simply
% uncomment this line.
[fitResults , gof]=fit([x,y],Vr,ft ,opts);

```

### A.3 Example of fitting function to get the amplitudes and phases.

```

function [amp12, clevel12]=fit12(t,U,W,old12)
%This function fits the 12 hour wave and a constant to the data set U based
%upon the weighting W and the time vector t. old12 was used as starting
%point for the amplitudes and phases unless they were too small/big, as
%this type needs to start in reasonable proximity of the true value in
%order to converge properly.
sigma=0.68;
k=1;
nans=0;
for i=1:length(t)
    if isnan(U(i));      %Finding the NaN's in the dataset.
        nans(k)=i;
        k=k+1;
    end
end

if antallPunkter(U)>=2*length(U)/3; %Checking that there are enough
    %datapoints.
    %antallPunkter is a short program which is basically the length of the
    %vector minus the number of NaN's in the vector.
FT=fittype('A12*cos(x*2*pi/12+phi12)+C', 'independent','x', 'dependent',...
'y');
opts = fitoptions( FT );
opts.Display = 'Off';
opts.Lower = [0 -inf -2*pi];
opts.Upper = [inf inf 2*pi];
opts.Weight=W;
if sum(nans)>0;%Could be anything, just checking for NaN's.
opts.exclude=excludedata(t,U,'Indices',nans); %Removing the NaN's if there
end                                     %are any.
if old12(1)>10&&old12(1)<70;
    opts.StartPoint = old12;
else
    opts.StartPoint=[30,0.5,0.5];
end
end
R=fit(t,U, FT, opts);
% figure(3)      %This would plot the data and the fit, so that I could see
% plot(t,U(:))  %if the program ran properly.
% hold on
% plot(R)
% hold off
amp12=coeffvalues(R);

```

```
clevel12=confint(R, sigma);  
else  
    amp12=[nan, nan, nan];  
    clevel12=[nan, nan, nan; nan, nan, nan];  
end
```